

06 / 07
NOVIEMBRE

IPG 2025
INTERNATIONAL PIPELINE GEOTECHNICAL CONFERENCE



Organizan:



Asociación
Colombiana
de Ingenieros

Probabilistic Approaches to Assessing Co-seismic Geohazard Risk for Oil and Gas Pipelines

Martin Zaleski and Adam Ballingall
BGC Engineering Inc.

06 de Noviembre de 2025

Agenda

- Project Objectives
- Background: Pipeline Failure in Earthquakes
- Project Setting: Location, Geology, Seismotectonics
- Methodology, Available Information, and Limitations
 1. Co-seismic geohazard inventory
 2. Shear strength model
 3. Stability analysis
 4. Probabilistic seismic hazard analysis
 5. Screening-level pseudo-probabilistic displacement analysis
 6. Probabilistic displacement hazard curves
 7. Pipe-soil interaction analysis and probability of pipeline failure
 8. Vulnerability, Consequence, and Risk
- Discussion and Limitations

Project Scope and Objectives

- Pipeline system: 1300 km total length, located in western Canada and northwestern US
- Recent system expansion provided extensive project-specific terrain maps, geotechnical information, and right-of-way construction information
- Objectives:
 1. Identify locations with relatively higher risk of loss of pipeline containment due to co-seismic geohazards, to prioritize risk reduction measures
 2. Estimate annualized risk of pipeline loss of containment due to co-seismic geohazards.
 3. Estimate annualized risk of system outage due to seismic effects on facilities (e.g., pump stations, tanks, etc.)
- This presentation focuses on Objectives 1 and 2: co-seismic landslides

Background

Pipeline Failure in Earthquakes

Strong Ground Shaking: transient compressive and shear stress on buried pipelines.

Liquefaction:

- **Settlement:** vertical bending
- **Lateral spreading:** Horizontal and vertical bending, and longitudinal compression and tension; depending on orientation of pipeline with respect to direction of movement

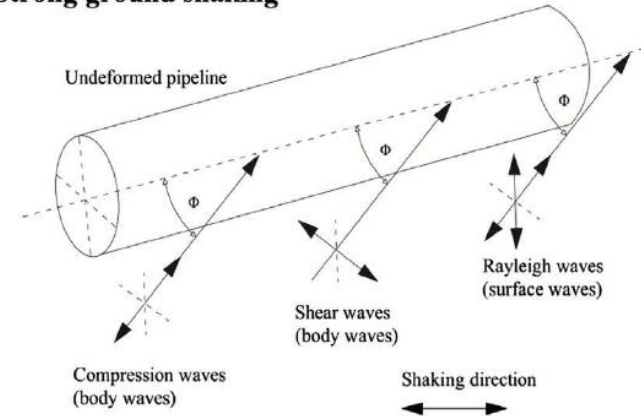
Landsliding: stress similar to lateral spreading, typically with larger magnitudes (pipelines embedded in non-liquefied soil)

Faults: bending, tension, or compression, depending on fault style and pipe orientation

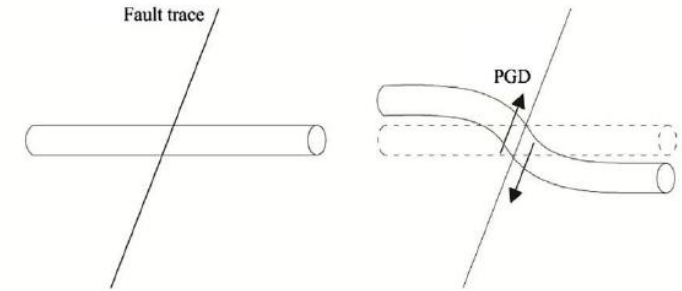
*This presentation covers the approach taken for **Co-Seismic Landsliding**.*

- *Liquefaction approach is similar and simpler, using the SDPM directly in place of a GMM*
- *Faulting and transient shaking were not part of the project scope*

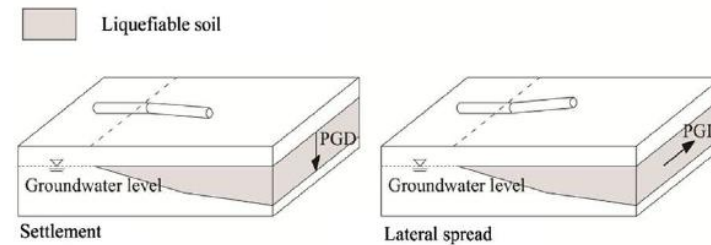
a) Strong ground shaking



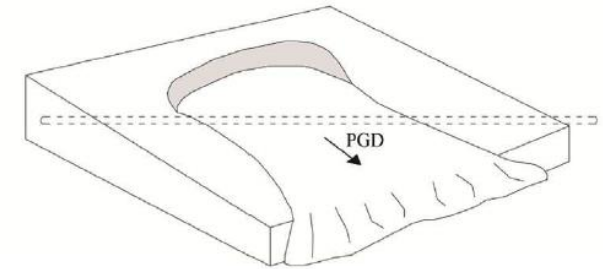
b) Fault displacement



c) Liquefaction



d) Earthquake-induced landslide

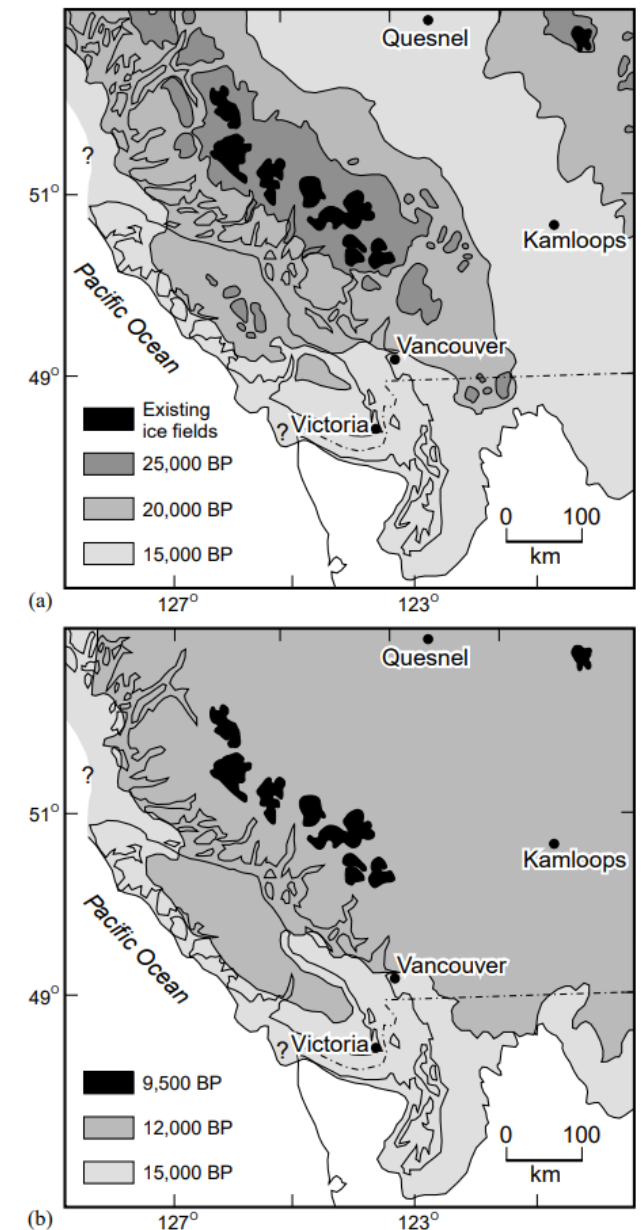


Source: Lanzano et al., 2014

Background

Geological Setting

- Variety of bedrock types with a range of shear strengths and landslide mechanisms
- Repeated Pleistocene glacial advances and retreats, culminating in the Fraser Glaciation between ~25 and ~9.5 ka
- Glaciation erased pre-existing geomorphic evidence for surface faulting and produced over-steepened mountains
- Diverse and complex surficial geological units related to glaciation, including:
 - Glaciofluvial deposits as terraces and outwash plains
 - Glaciolacustrine deposits in ice-dammed lakes
 - Glaciomarine deposits around isostatically-depressed paleo-shorelines
 - Basal and ablation till
 - Colluvium related to postglacial gravitational processes and landsliding



Source: Clague and James, 2002

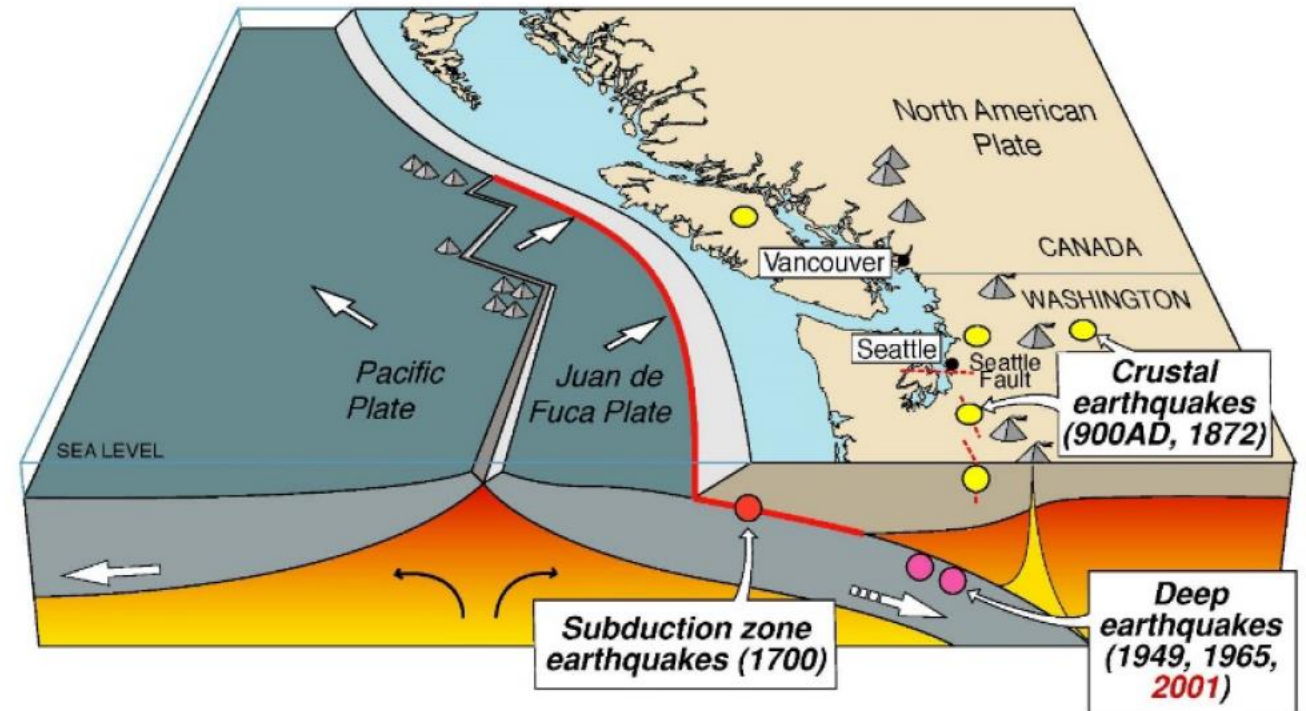
Background

Seismotectonic Setting

Study region experiences increasing seismic hazard toward the west coast of North America.

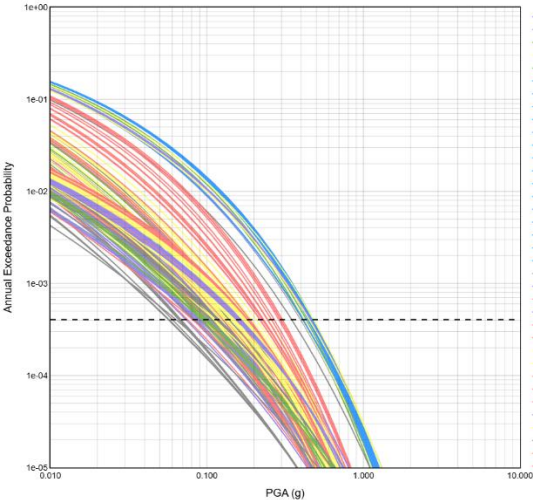
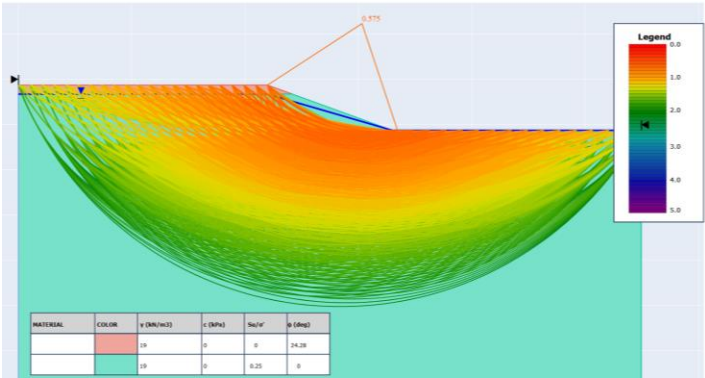
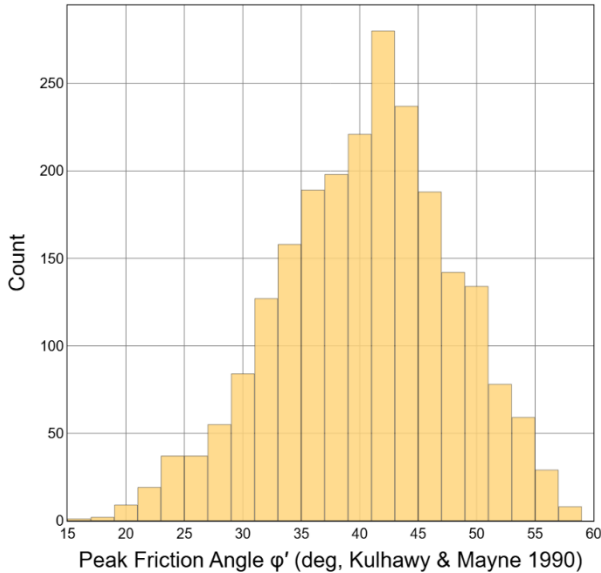
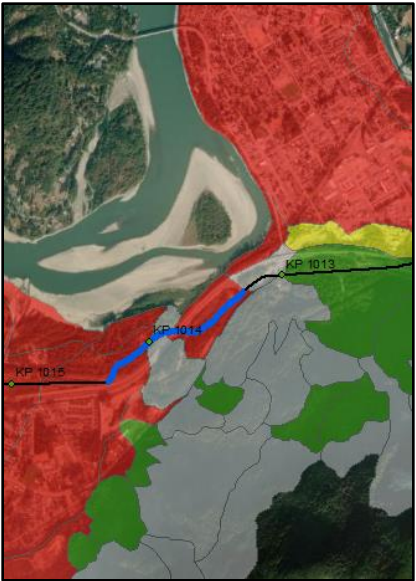
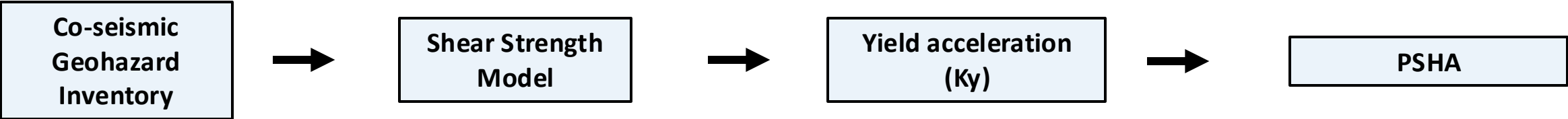
Three earthquake source types:

- Megathrust plate-boundary earthquakes up to M~9
- Frequent, deep in-slab earthquakes up to M~8
- Shallow crustal earthquakes in forearc region up to M~7.6. Limited information on crustal faults: slow strain rate and glacial masking of geomorphology

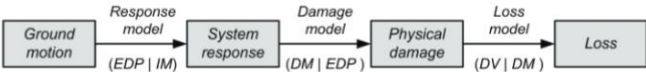
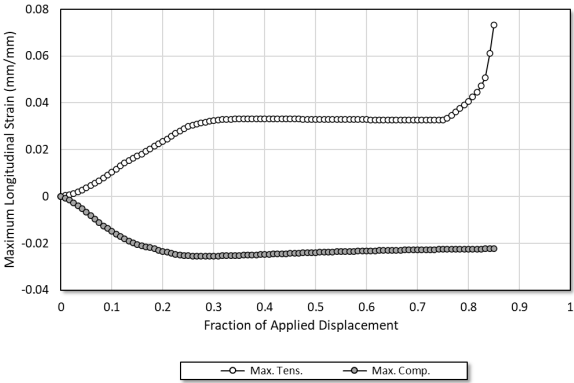
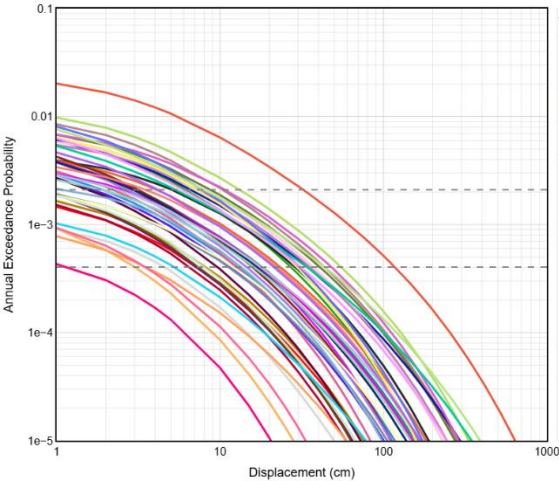
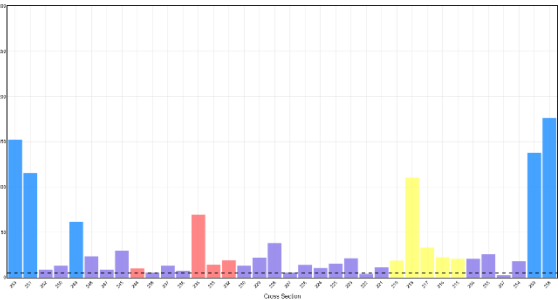
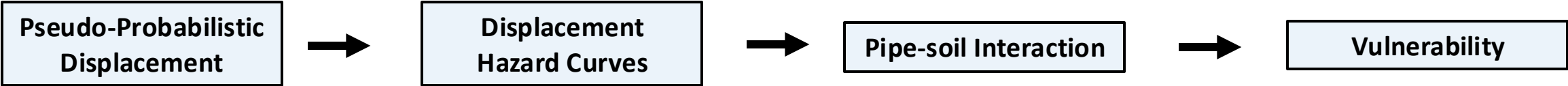


Source: USGS

Project Methodology – Co-Seismic Landslides

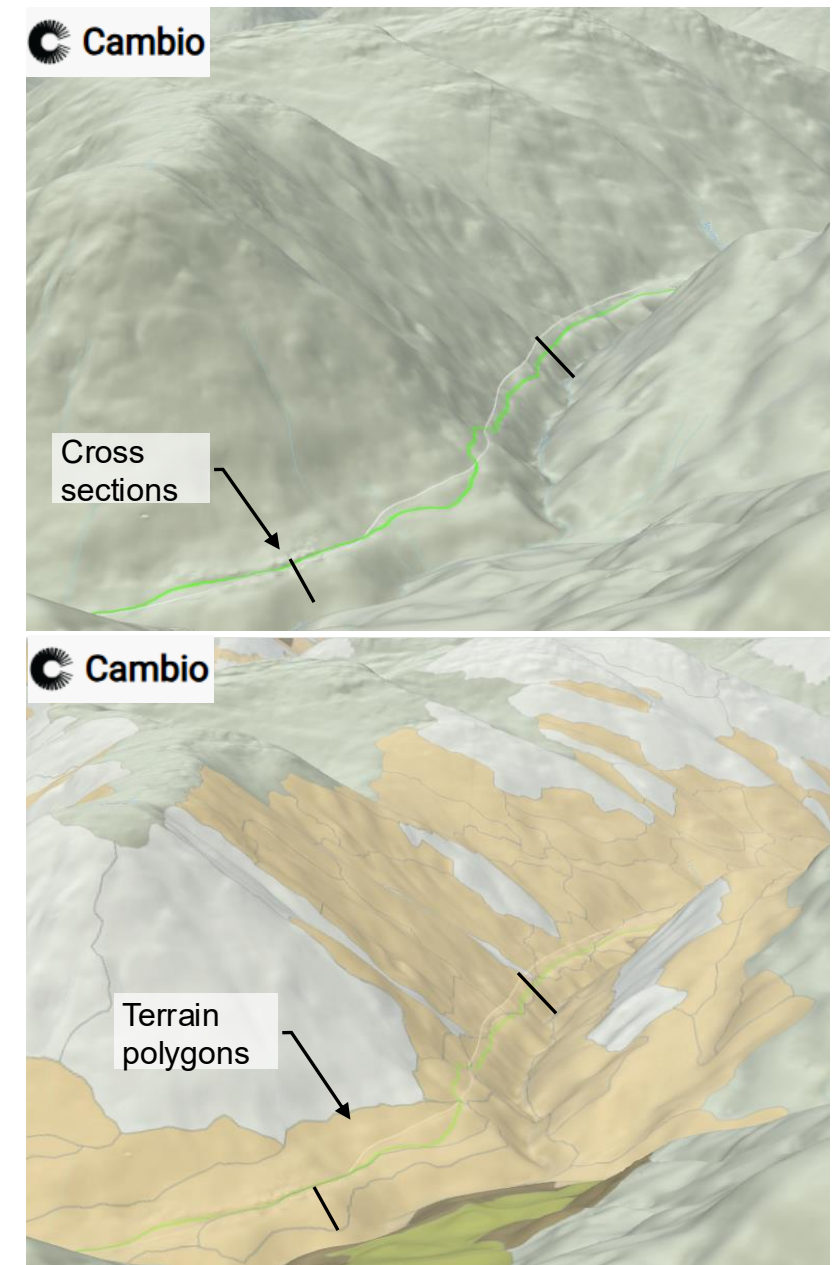


Project Methodology – Co-Seismic Landslides



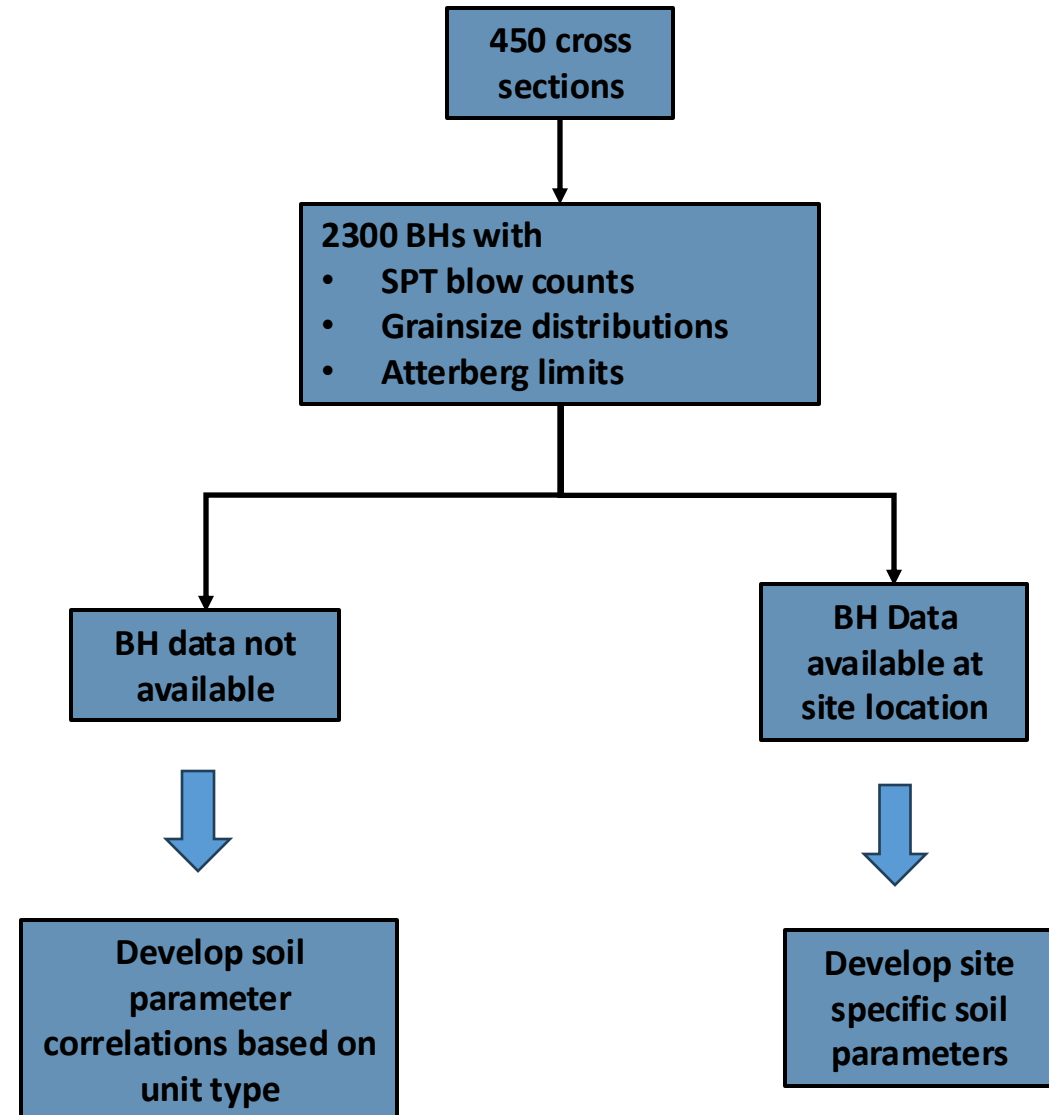
Co-Seismic Geohazard Inventory

- Project-specific terrain mapping performed to delineate surficial geological units
- ~450 representative cross sections drawn to analyze co-seismic landslides
- ~300 lateral spreading sites delineated based on liquefaction susceptibility classification and presence of adverse topography (proximity to free faces or sloping terrain)



Shear Strength Model

- Challenge:
 - Estimate soil parameters across large spatial extents and different geological material types and deposition environments
 - Soil strengths needed for stability modelling
 - V_{s30} needed for seismic hazard
- Majority of sites did not have available BH data



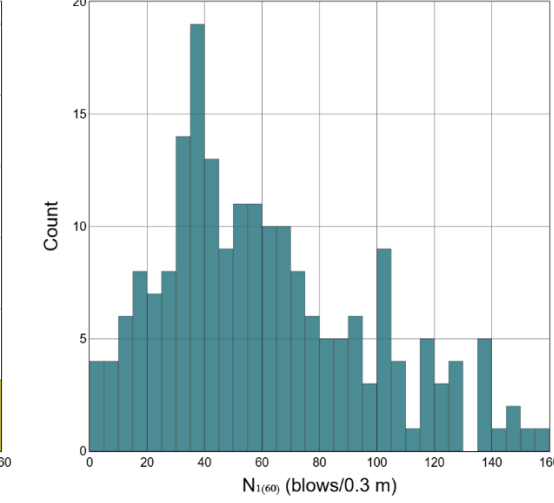
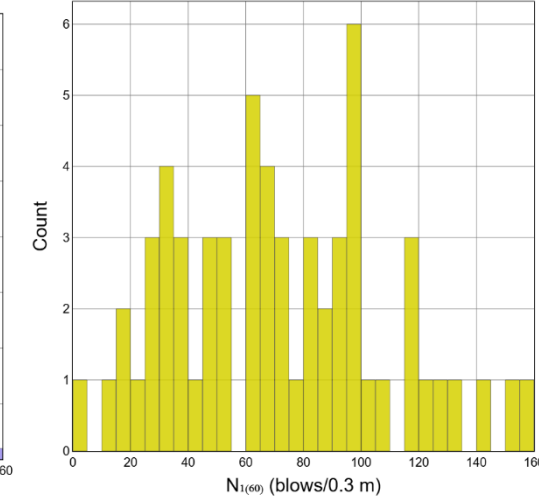
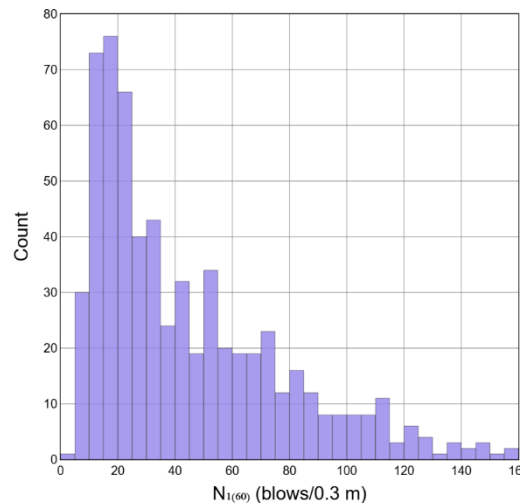
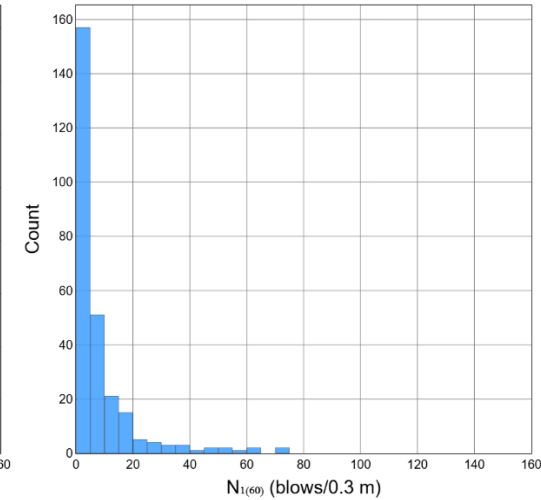
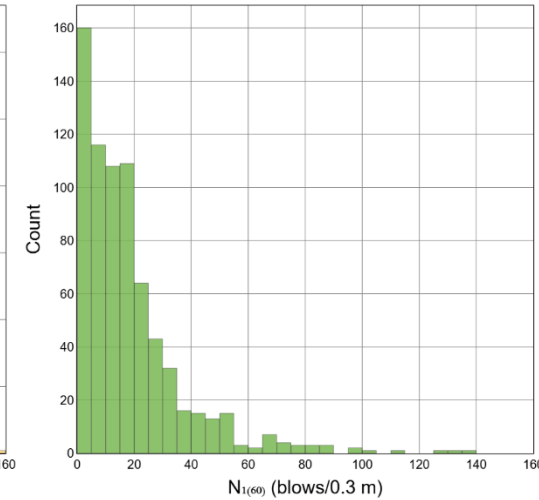
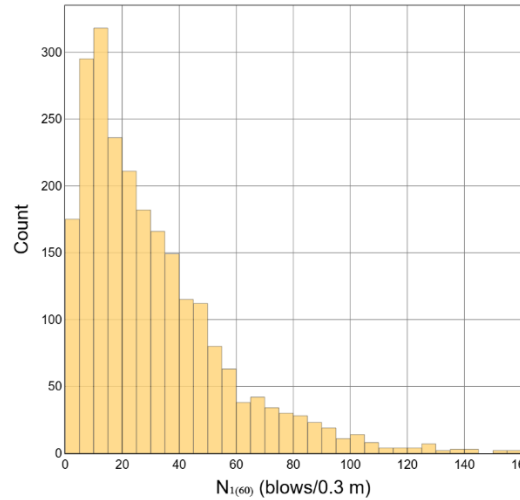
Shear Strength Model

SPT N-Value Distributions

- Grouped genetic units (bedrock and glacial/postglacial deposits) into comparable behaviour classes
- Plotted $N_{1(60)}$ from borehole data for each group

Unit Types

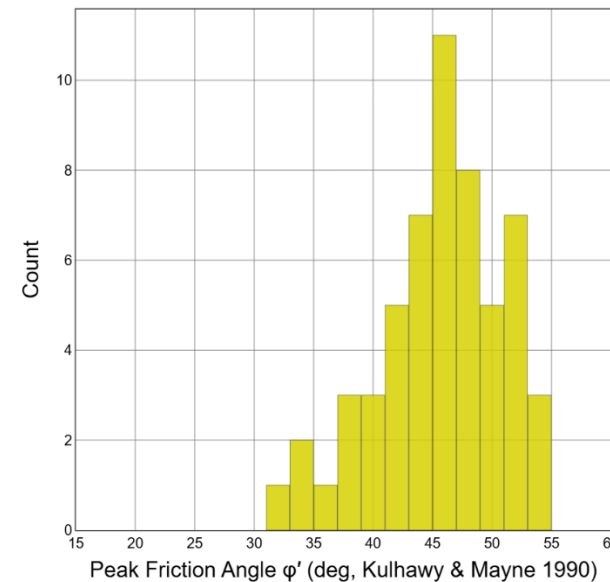
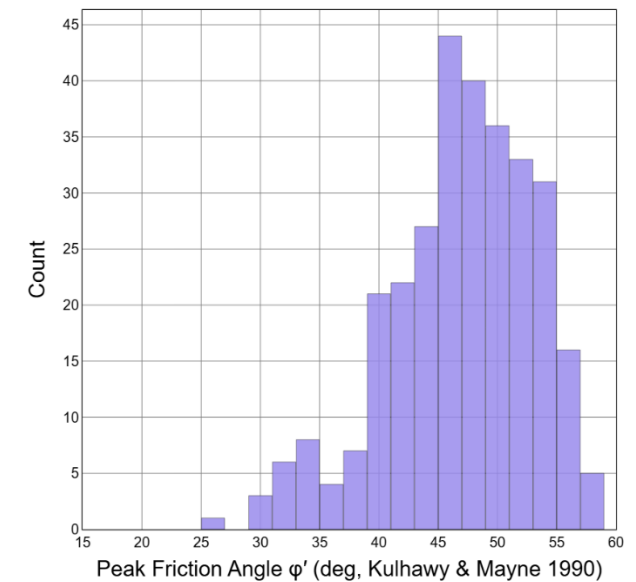
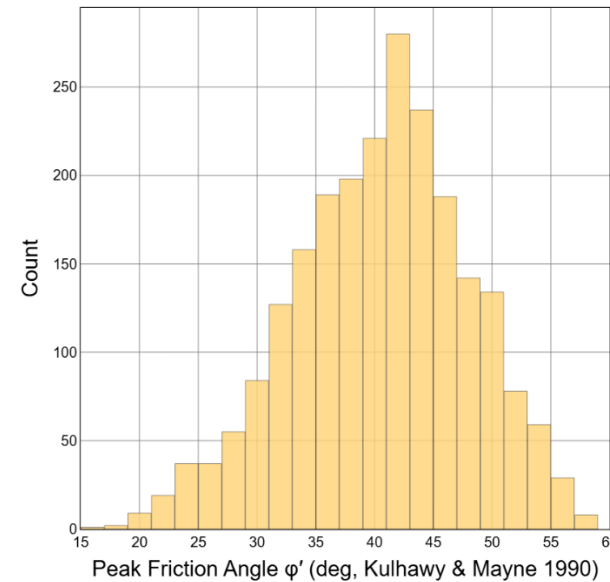
- Fluvial +
Recessional glaciofluvial +
Colluvium
- Lacustrine +
Recessional glaciolacustrine
- Recessional glaciomarine
- Till
- Advance glaciofluvial
- Advance glaciolacustrine +
Advance glaciomarine



Shear Strength Model

Coarse-grained unit types:

- Estimated effective friction angles (ϕ') using empirical correlations with SPT blow counts
- Friction angle histogram developed for each coarse-grained group



Friction Angle Histograms

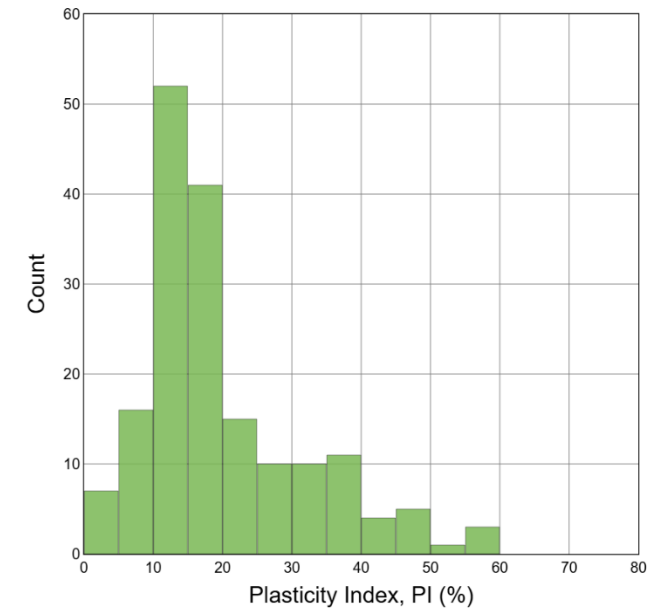
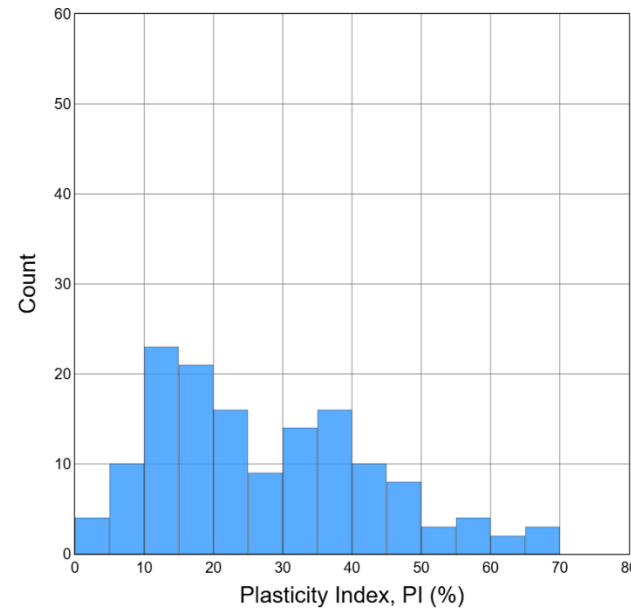
Unit Types

- Fluvial +
- Recessional glaciofluvial + Colluvium
- Till
- Advance glaciofluvial

Shear Strength Model




Fine-Grained Units

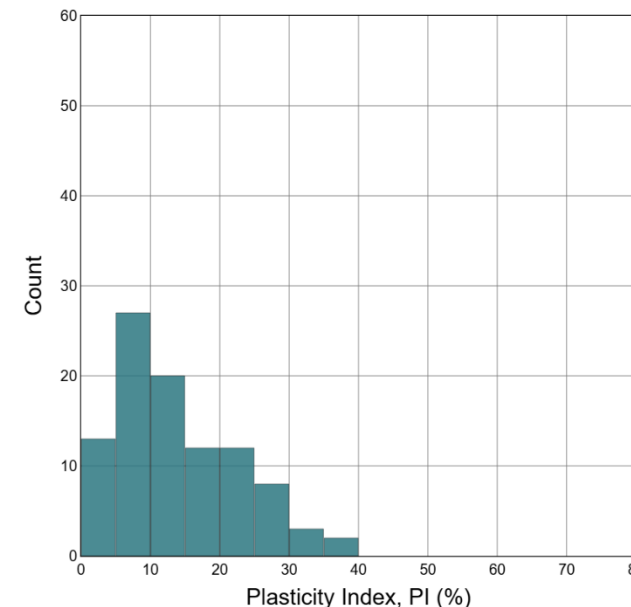
- Used empirical correlations with Atterberg Limits to estimate (ϕ') and undrained shear strength ratios (S_u/σ'_v)
- Drained strength used above the water table, while undrained strength was used below the water table



Plasticity Index Histograms

Unit Types

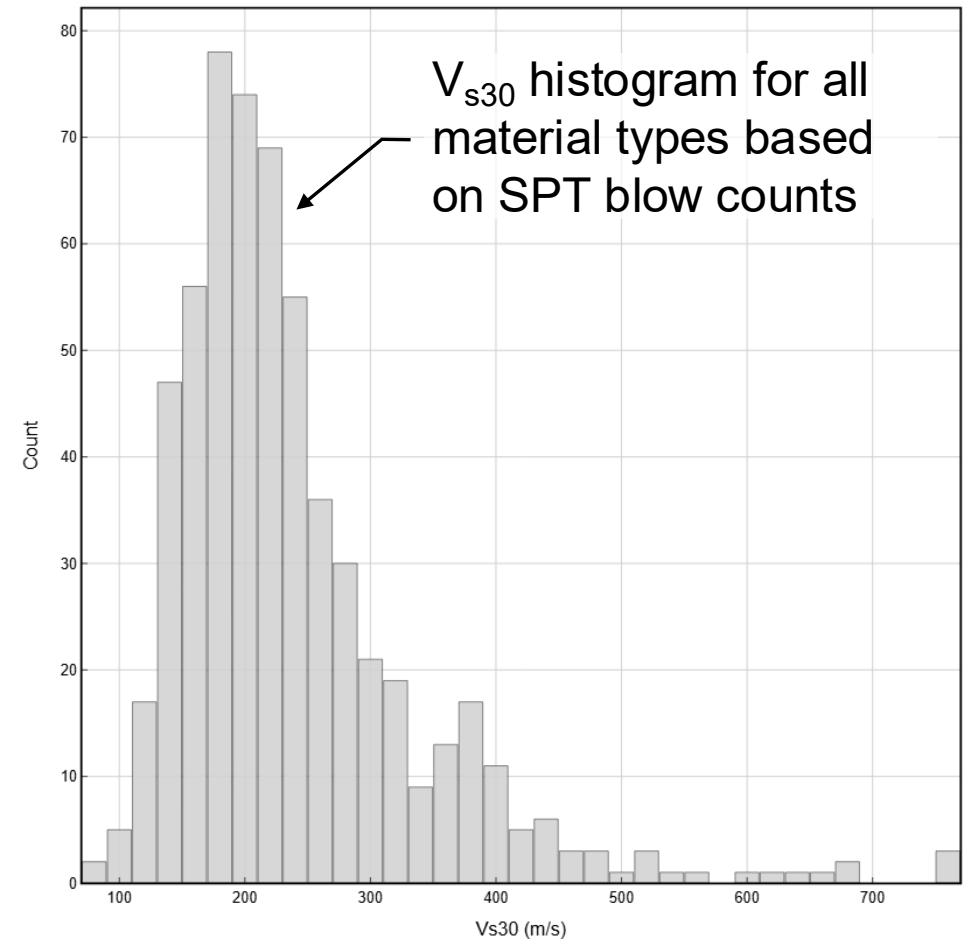
-  Lacustrine + Recessional glaciolacustrine
-  Recessional glaciomarine
-  Advance glaciolacustrine + Advance glaciomarine



Seismic Site Characterization Model

Shear Wave Velocity – V_{s30}

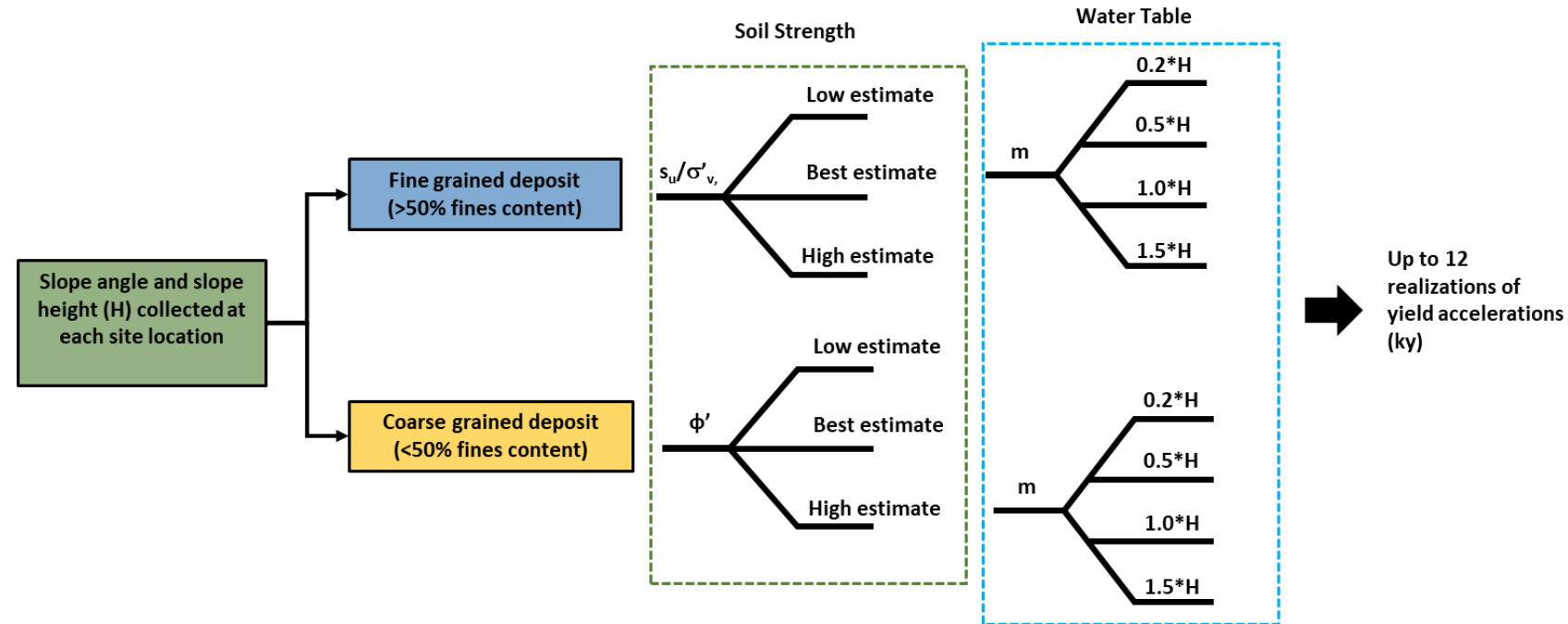
- Used empirical correlations with SPT N-values (Wair et al., 2012) to develop V_{s30} histograms by unit type



Slope Stability Analysis

Logic Tree Approach for Shear Strength and Groundwater Level

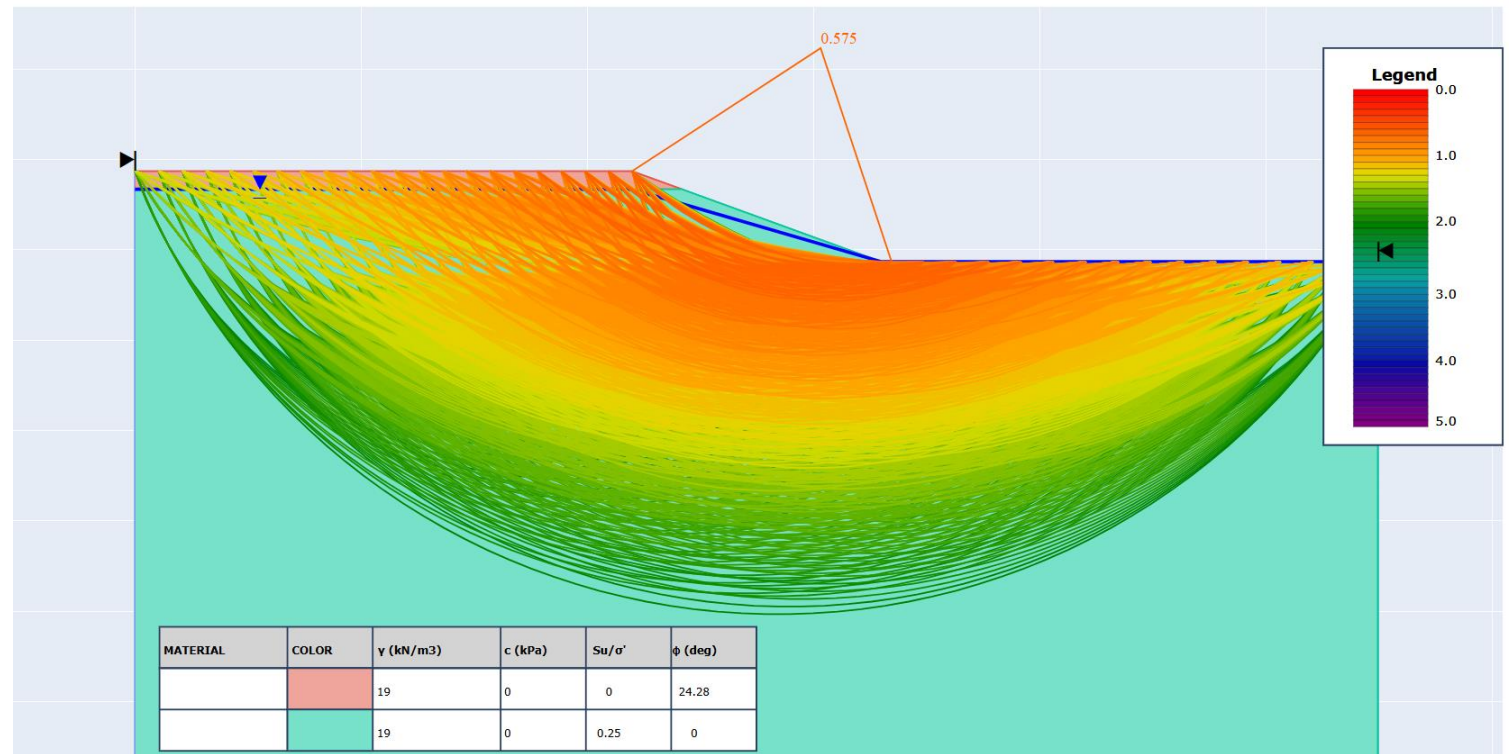
- Challenge: managing uncertainty at sites without input parameters defined by site-specific geotechnical study
- Solution: Incorporate epistemic uncertainty using logic trees (Ojomo et al., 2024)



Slope Stability Analysis

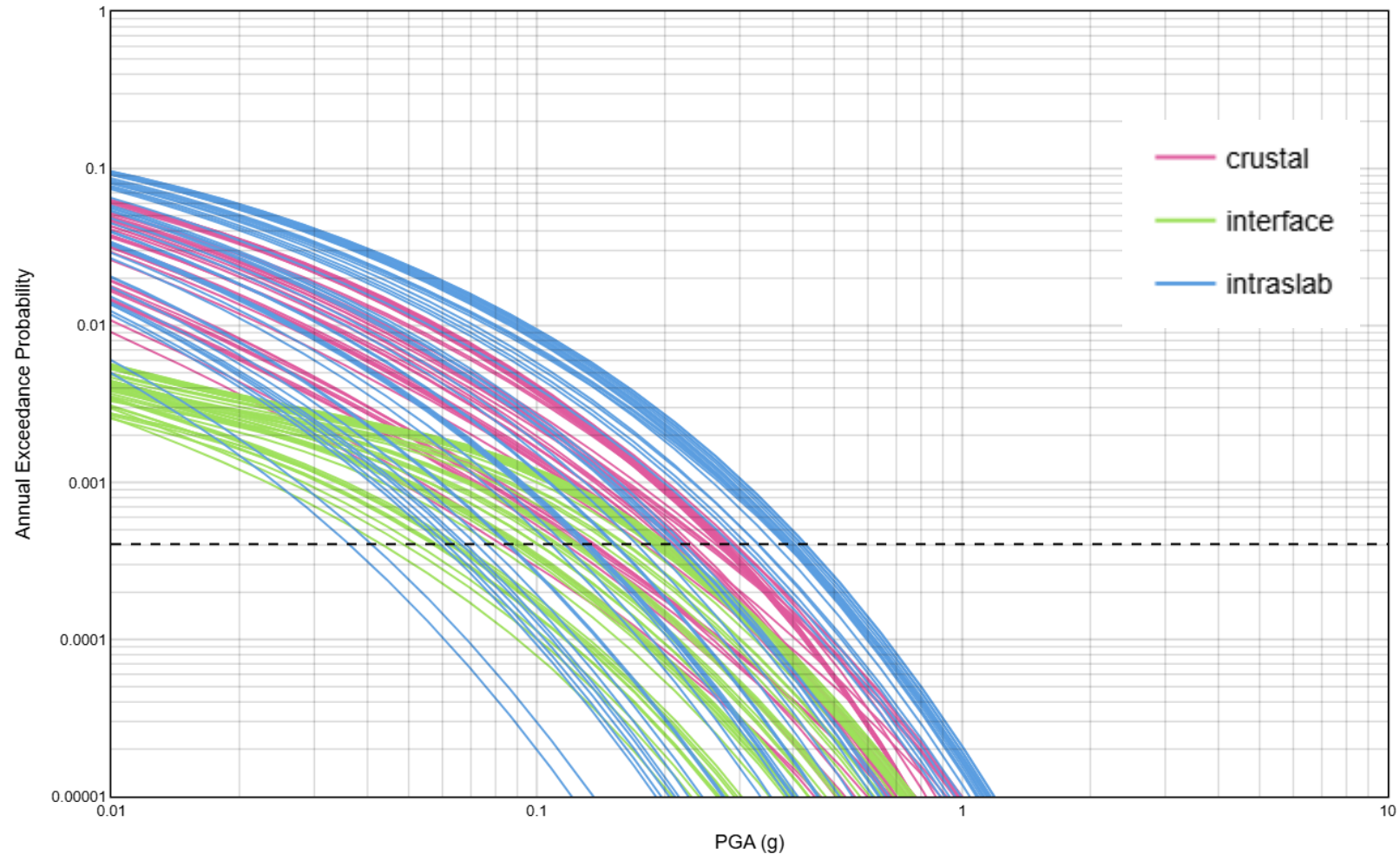
Yield Acceleration - Ky

- Performed stability analysis for each realization of the logic tree
- Used open-source, python-based LE modeling software with modifications
- Ky derived from static FOS



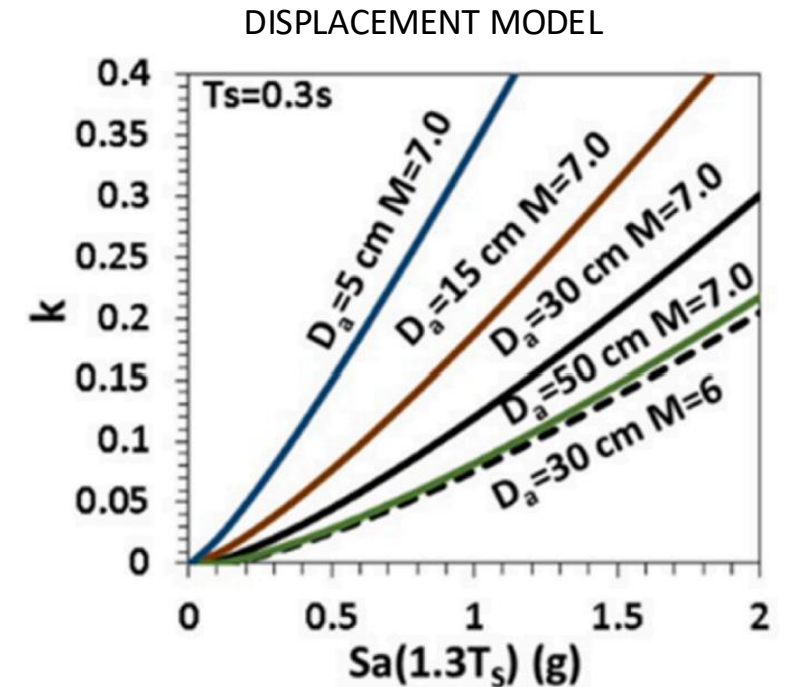
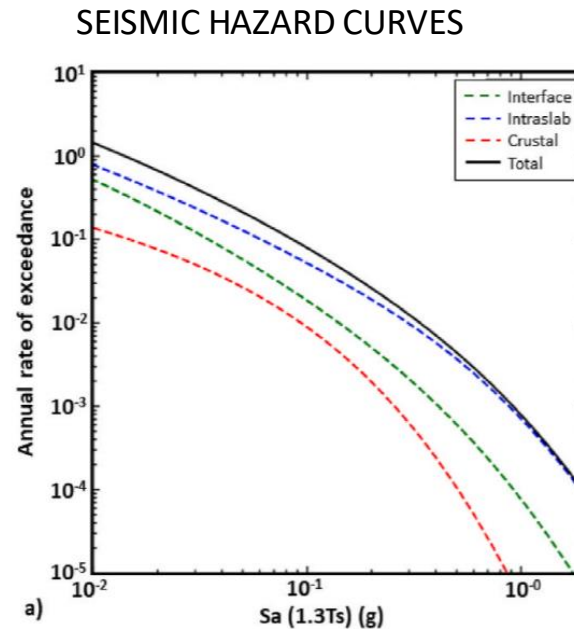
Probabilistic Seismic Hazard Analysis

- PSHA performed at each site with V_{s30} derived from unit type
- Source and ground motion models derived from the following:
 - Canada: NRCAN 6th Generation (2020) model, implemented in OpenQuake
 - USA: USGS NSHM 2023 model, implemented in NSHMP-HAZ
- Disaggregations by tectonic region type, magnitude, distance



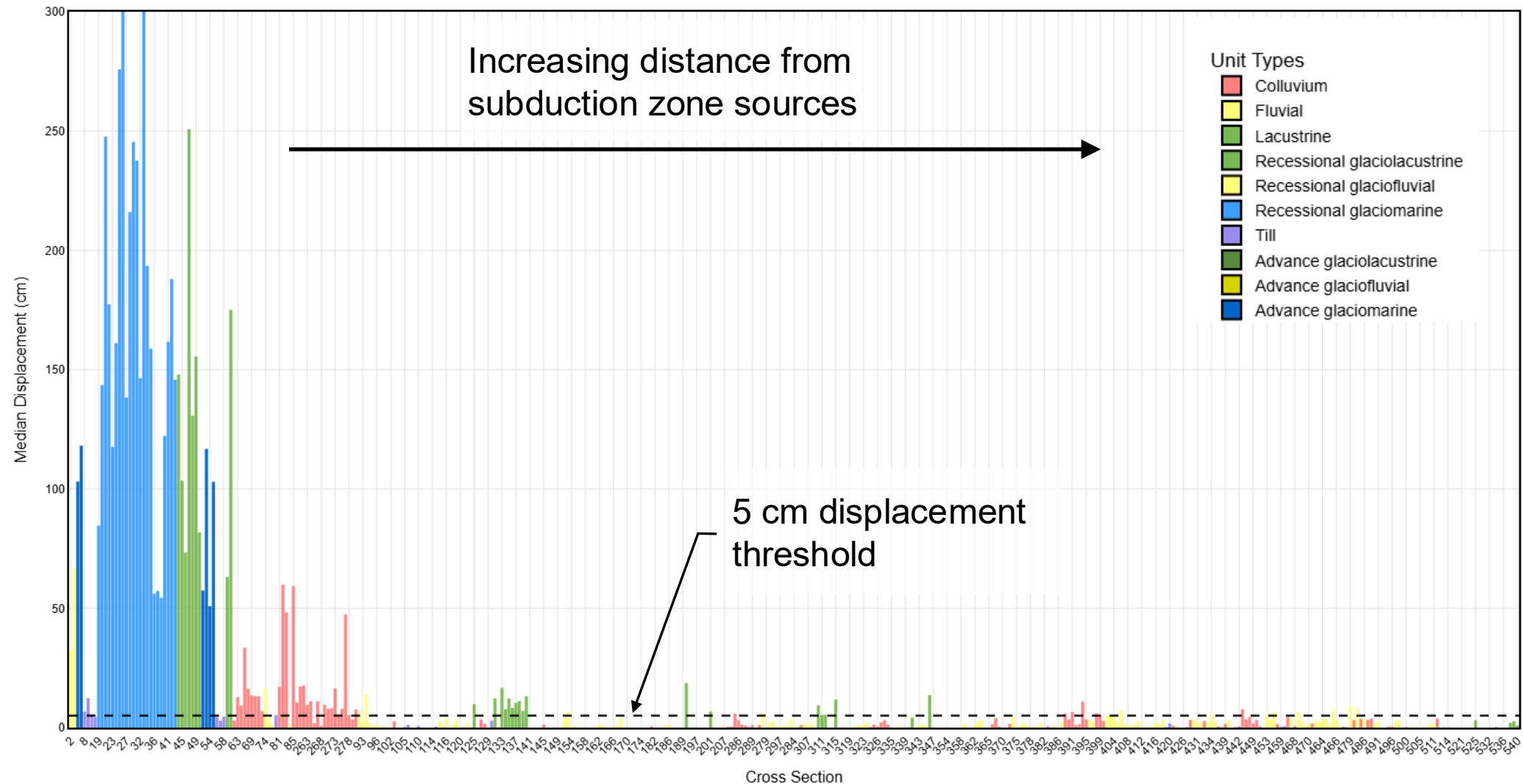
Pseudo-Probabilistic Displacement Analysis

- Employed ***hazard frequency*** approach: displacement for a specified exceedance probability
- 2%-in-50-year ground-motion level and M obtained from disaggregations
- Applied SDPM as follows:
 - Crustal: Bray & Macedo, 2019
 - Interface and intra-slab: Macedo et al., 2023
- Slopes with median displacement <5 cm were removed from further consideration



Source: Bray & Macedo 2020

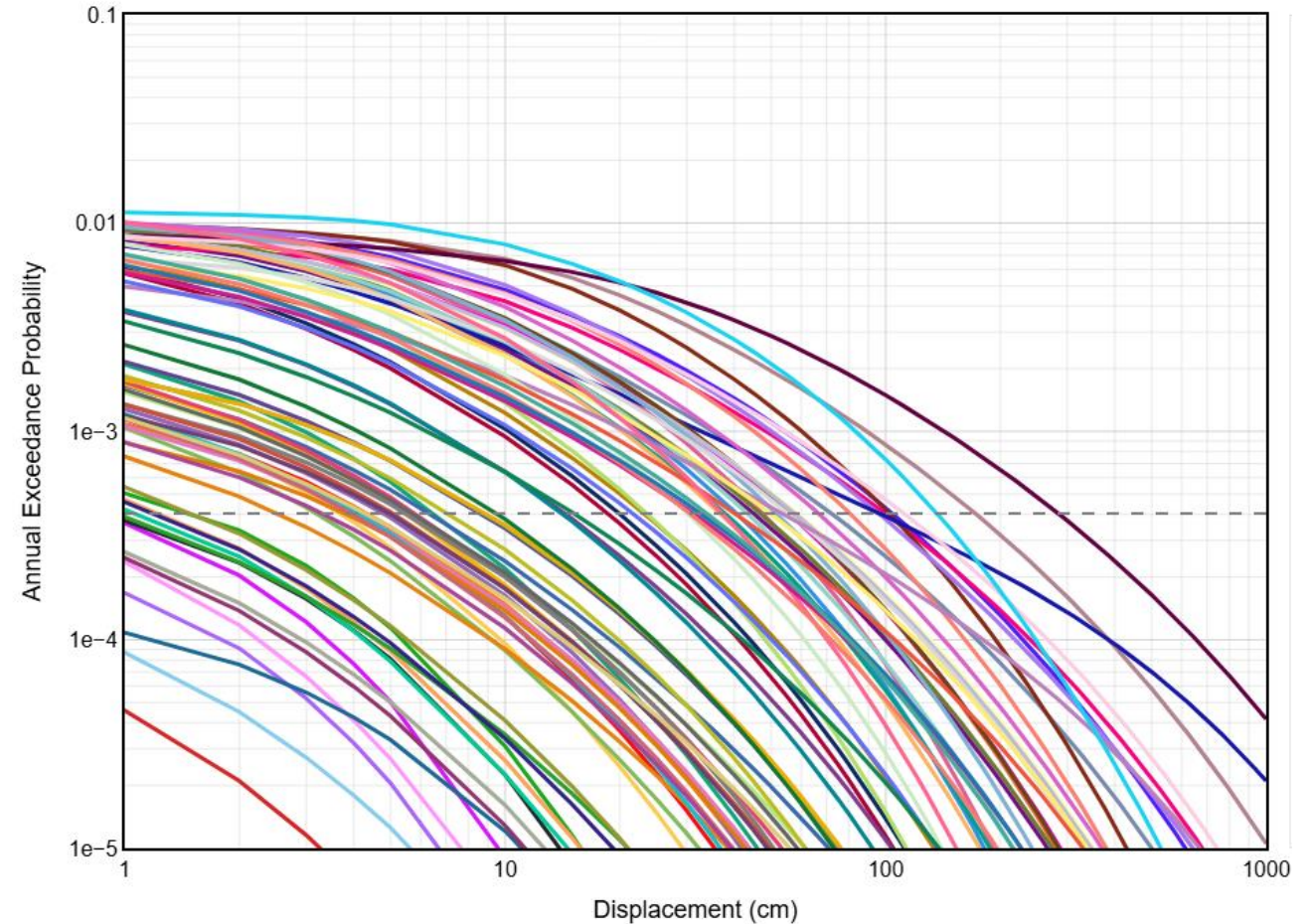
Pseudo-Probabilistic Displacement Analysis



Probabilistic Displacement Hazard Curves

Problem:

- Displacement hazard curves are developed for each cross section passing the screening level assessment.
- Challenges:
 - SDPM require both $S_a(1.3T_s)$ and M as inputs: cannot substitute directly for a GMM in a PSHA framework.
 - Different SDPM apply to different tectonic regions:
 - Crustal: Bray & Macedo 2019
 - Subduction: Macedo et al. 2023

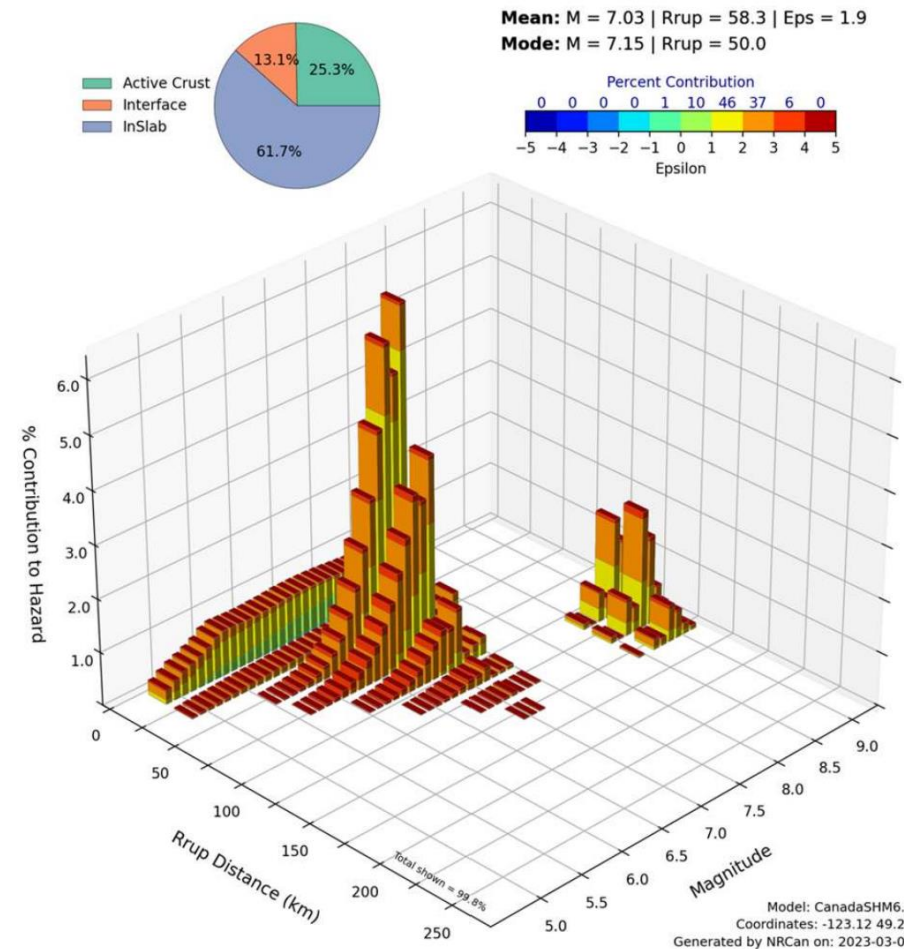


Probabilistic Displacement Hazard Curves

Solution:

1. **Disaggregate** total hazard at fixed exceedance probabilities to obtain distribution of M by tectonic region type
2. **Compute $P(D > d \mid IM, TRT, M)$:**
 - For each TRT and M , apply TRT-specific SDPM
 - $IM = Sa(1.3Ts)$ from that TRT's component hazard curve
3. **Compute $P(D > d \mid IM)$:**
 - Sum all $P(D > d \mid IM, TRT, M)$, weighted by M - TRT proportional contribution.
4. **Repeat** for a range of threshold d values.
5. **Repeat** for each exceedance probability to construct displacement hazard curve.

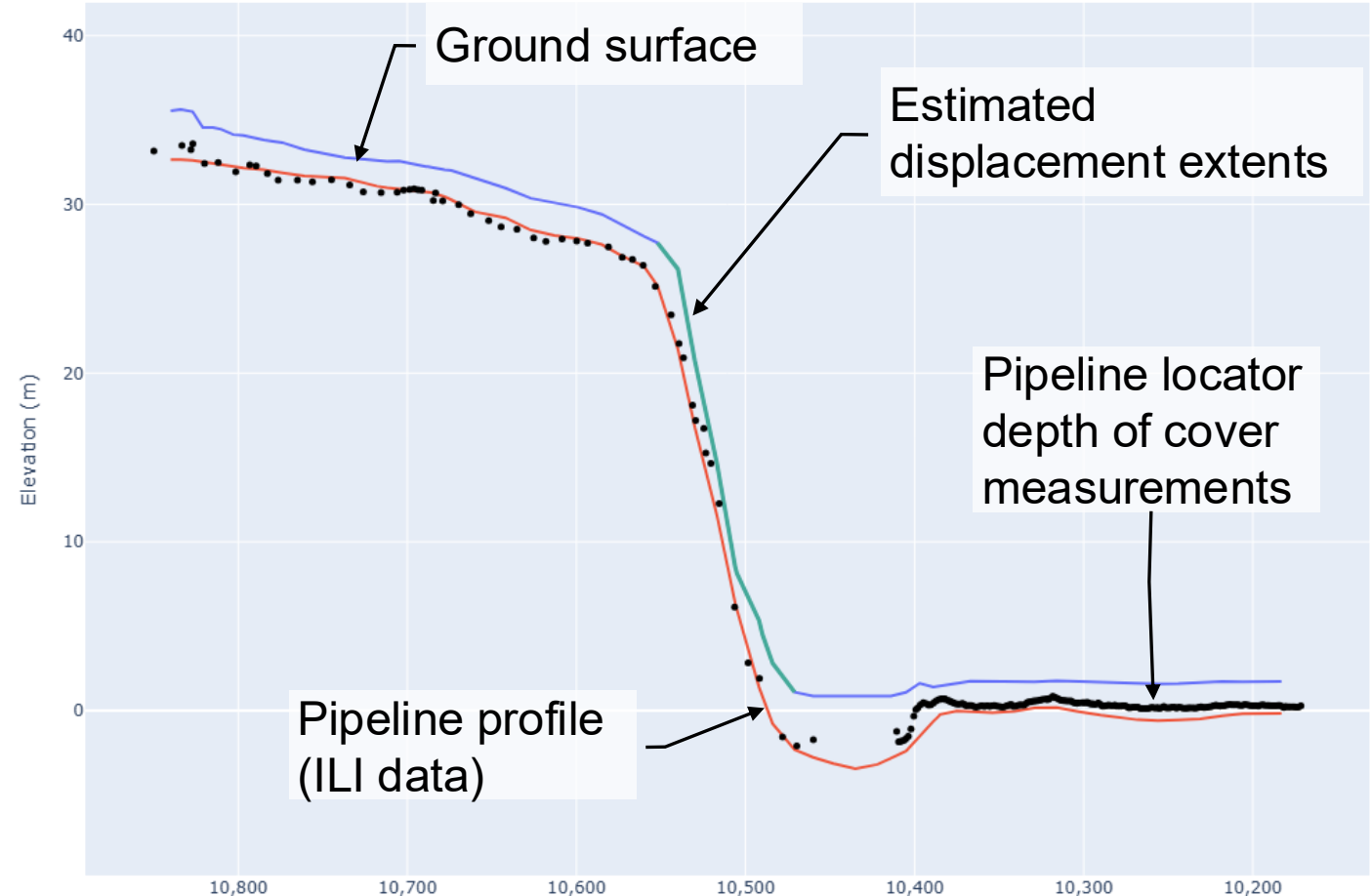
Example M-R-TRT- ξ disaggregation from a site in SW BC.
Source: Kolaj et al., 2023



Pipeline Strain Response and Probability of Failure

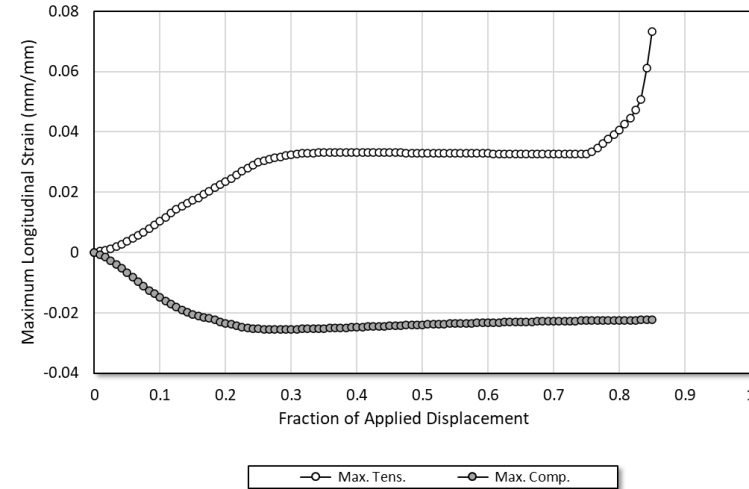
- At each location, estimate displacement extents relative to pipeline profile and alignment
- Worked with a pipe-soil interaction specialist to inform the strain response and probability of failure for the pipeline at selected locations

Example of pipeline profile for one site

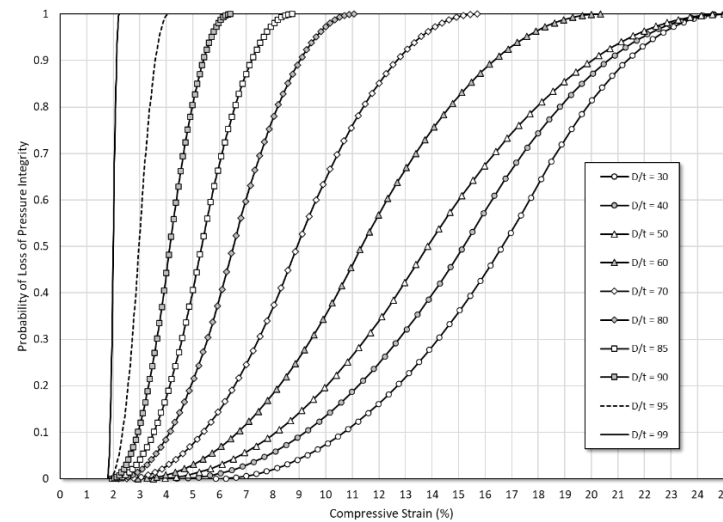


Pipeline Strain Response and Probability of Failure

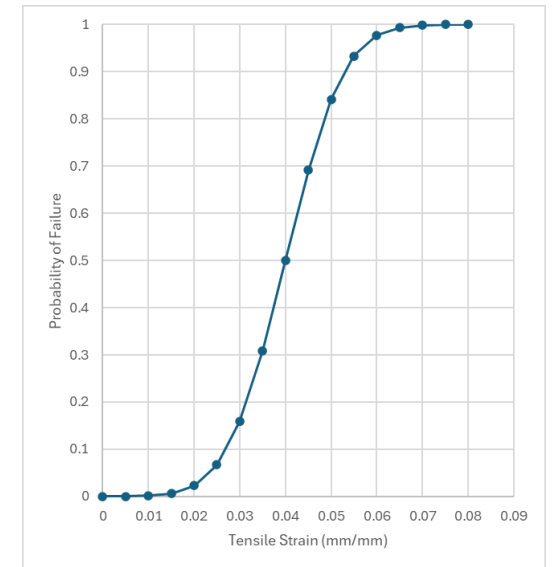
- Delineated ~130 sites for the vulnerability assessment
- In-line-inspection (ILI) data used to inform:
 - Pipeline geometry (alignment and profile)
 - Pipeline material properties (wall thickness, diameter, steel grade, operating pressure)



Compression strain capacity



Tensile strain capacity



Vulnerability, Consequence, and Risk

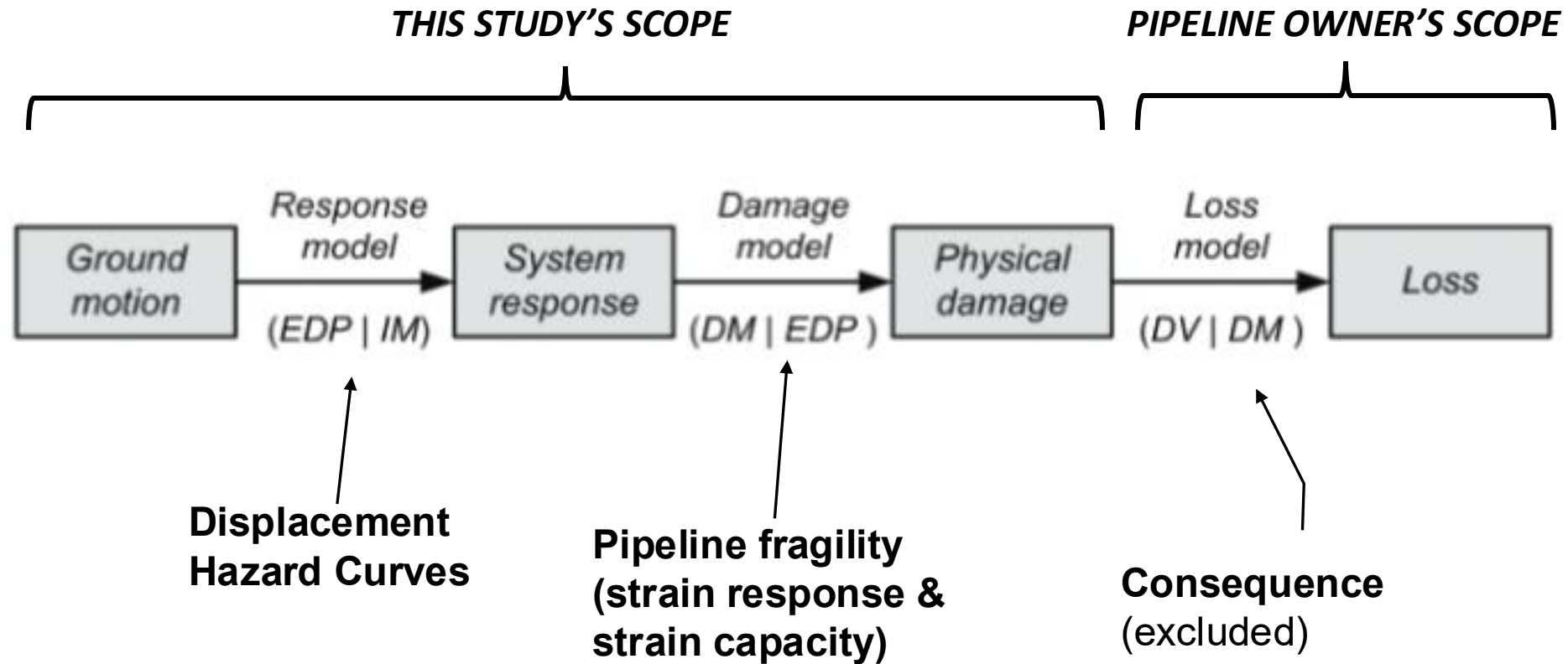


Image modified from Kramer & Stewart (2024)

Discussion and Limitations

- Screening-level pseudo-probabilistic approach can short-list sites with credible damage potential with relatively low effort
- Probabilistic approach is best suited to a subset of higher-priority sites, each using location-specific pipeline fragility functions (pipe-soil interaction analyses)
- Logic-tree approach implies that site-by-site risk estimates may be inaccurate compared with those obtained from site-specific geotechnical studies, but the aggregate risk estimate over all sites on the pipeline system is expected to be reliable.
- Highest-risk sites would benefit from site-specific geotechnical study (reduce epistemic uncertainty in shear-strength model) and/or stability/displacement models (replacing assumed uniform geology)

Contact us

Martin Zaleski

Principal Engineering Geologist

mzaleski@bgcengineering.ca

bgcengineering.ca



BGC Locations

CANADA

VICTORIA

VANCOUVER

KAMLOOPS

KELOWNA

CALGARY

EDMONTON

TORONTO

SUDBURY

KINGSTON

OTTAWA

MONTREAL

QUEBEC CITY

HALIFAX

FREDERICTON

DOMINICAN REPUBLIC

SANTO DOMINGO

USA

GOLDEN

NASHVILLE

AUSTRALIA

BRISBANE

CHILE

SANTIAGO

IPG2025-036

PROBABILISTIC APPROACHES TO ASSESSING CO-SEISMIC GEOHAZARD RISK FOR OIL AND GAS TRANSMISSION PIPELINES

Martin Zaleski
BGC Engineering Inc.
Vancouver, Canada

Adam Ballingall
BGC Engineering Inc.
Vancouver, Canada

Yolanda Alberto
BGC Engineering Inc.
Toronto, Canada

Daniela Welkner
BGC Engineering Inc.
Santiago, Chile

ABSTRACT

Pipelines in seismically active regions face numerous threats, including transient wave propagation, liquefaction, landsliding, and surface fault rupture. Effective management of these seismic hazards is crucial for ensuring the integrity and safety of oil and gas transmission pipelines. This paper presents state-of-practice methodologies for both screening-level pseudo-probabilistic and system-wide fully probabilistic co-seismic geohazard assessment. These methodologies provide operators with cost-effective tools for prioritizing risk reduction measures.

The first step involves inventorying pipeline crossings of potentially active faults and terrain susceptible to co-seismic liquefaction and landslides. A logic-tree approach is employed to incorporate epistemic uncertainty in geotechnical parameters along a pipeline system. Pseudo-probabilistic approaches apply seismic displacement prediction models to estimate displacement at a target exceedance-probability level or the frequency of exceeding a displacement threshold. Fully probabilistic approaches integrate seismic hazard curves and displacement prediction models to develop displacement hazard curves at each co-seismic geohazard crossing. These curves are combined with fragility models, obtained from empirical data or finite-element analyses, to estimate annualized rupture frequency at each crossing, which may be summed to estimate total system co-seismic rupture frequency.

By integrating screening-level and probabilistic analyses, this framework enables operators to estimate failure frequencies and focus risk reduction measures more effectively. This approach not only enhances the understanding of seismic risks but also contributes to the development of more resilient pipeline systems, ultimately improving the safety and reliability of the onshore oil and gas pipeline industry.

Keywords: seismic risk, liquefaction, co-seismic landslide, probabilistic analysis, seismic displacement hazard curves

NOMENCLATURE

λ	annual rate of exceedance
AEP	annual exceedance probability
a_c	critical acceleration
D	displacement
DHC	displacement hazard curve
DV	decision variable
EDP	engineering demand parameter
IM	intensity measure
k_y	yield acceleration
L	loading parameter
M	magnitude
PGA	peak ground acceleration
PGD	permanent ground displacement
PGV	peak ground velocity
PRCI	Pipeline Research Council International
PSHA	probabilistic seismic hazard analysis
R	distance to the source
S	site parameters
SDPM	seismic displacement prediction model
TGD	transient ground displacement
T_s	fundamental period
UHRS	uniform hazard response spectra
USGS	United States Geological Survey
V_s	shear wave velocity
w	weight

1. INTRODUCTION

This paper outlines a methodology for the development of seismic displacement hazard curves (DHCs) at pipeline crossings of terrain with credible potential for co-seismic ground failure, as a requisite input into pipeline risk analyses. The general approach involves:

- Identifying locations with susceptibility to co-seismic ground failure
- Performing seismic hazard analysis to obtain hazard curves and disaggregations of the hazard by magnitude and tectonic region type
- Developing representative soil shear strength models that incorporate logic trees to capture a range of credible shear-strength values and groundwater levels for mapped geological deposit type
- Performing screening-level analysis using semi-empirical and empirical seismic displacement prediction models (SDPMs) for landsliding and triggering analysis for liquefaction
- Developing DHCs by integrating seismic hazard curves and SDPMs for liquefaction and lateral spreading that incorporate relative contributions of crustal and subduction earthquakes

The work described herein is part of a system-wide seismic hazard analysis for a pipeline corridor in western Canada. It will be combined with site-specific fragility curves developed using finite element modelling, to incorporate local variation in burial depth, pipeline orientation with respect to ground movement, length of pipe embedded in moving ground, and other site-specific mechanical and geometric considerations. This paper is limited to the SDPM component of the scope; subsequent work will integrate fragility models to develop total annual pipeline failure probability estimates and prioritize crossings on a risk basis for seismic risk reduction efforts. Probabilistic and pseudo-probabilistic approaches to estimating co-seismic ground failure hazard are described.

2. BACKGROUND

2.1. Pipeline Vulnerability to Seismic and Co-Seismic Hazards

Buried pipelines can lose serviceability or product containment during earthquakes as a direct result of transient stress changes arising from seismic wave propagation or the indirect effects of co-seismic permanent ground displacement (PGD) due to fault displacement, liquefaction, or landsliding [1, 2, 3] (Figure 1). Temporary displacement of soil caused by the propagation of seismic waves is referred to as transient ground deformation (TGD); the damaging effects of TGD are generally proportional to the Peak Ground Velocity (PGV) of the passing seismic waves [4]. Ground surface displacement caused by surface faulting, liquefaction, or earthquake triggered landslides is referred to as permanent ground deformation (PGD). Co-seismic liquefaction and landslide triggering is generally proportional to the peak ground acceleration (PGA). Case-history information from global earthquakes shows that PGD has accounted for more pipeline incidents than TGD [4].

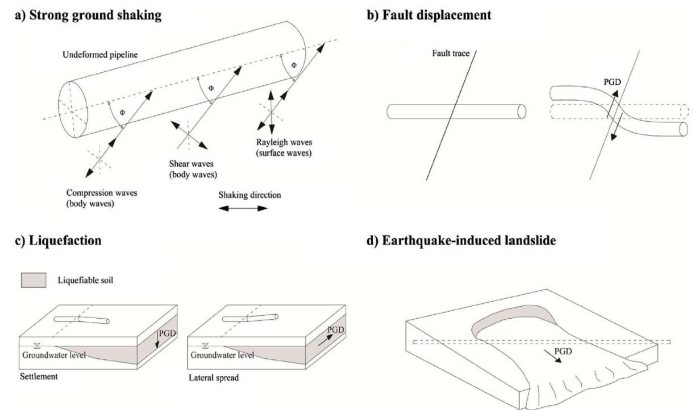


FIGURE 1: PIPELINE FAILURE MECHANISMS IN EARTHQUAKES. FROM [2].

Surface fault rupture typically occurs along or near geological faults with documented historical and/or prehistorical activity [5]. Surface fault rupture hazard is therefore higher in active tectonic areas and where Quaternary faults are present.

Liquefaction may occur where loose, saturated soils are subjected to strong earthquake shaking, causing a sudden increase in pore-water pressure, decrease in effective stress, and loss of shear strength. Liquefaction probability increases with PGA and is possible in susceptible soils where PGA exceeds 0.09 g [6]. PGD caused by liquefaction has been observed in $M > 4.5$ earthquakes [7, 8]. Pipeline integrity impacts are rare where liquefaction manifests as settlement or sand boils, but more common in lateral spreads and flows triggered by liquefaction [9]. Liquefaction susceptibility is related to geologic age and depositional environment [10, 11]. PRCI design guidelines recommend that the design of most pipeline projects consider liquefaction where they cross sedimentary deposits with high or very high liquefaction susceptibility [12].

Co-seismic landslides can occur where PGA experienced in an earthquake exceeds a slope's critical acceleration (a_c), which is the horizontal acceleration required to reduce the factor of safety against sliding below unity. At a given location, screening-level a_c may be calculated using an infinite-slope pseudostatic limit-equilibrium model [13, 14]. A magnitude threshold for PGD related to earthquake triggered landslides and surface faulting is approximately $M_w 5.0$ [15, 16, 5].

2.2. Project Context and Description

The subject of the work was a pipeline corridor through the Western North American Cordillera. Seismic hazard is relatively high near the Pacific Ocean shoreline of the study region, owing to its proximity to the Cascadia Subduction Zone. The forearc region, west of the Coast Mountains, is subject to periodic megathrust earthquakes with magnitudes up to about 9, frequent intraslab earthquakes deep below ground surface within the down-going Juan de Fuca plate, and strong earthquakes on crustal faults in the overriding Pacific Plate where oblique subduction causes forearc compression and deformation (Figure 2). Seismic hazard is moderate through the Rocky Mountains but

low through the central Cordillera and in the Plains east of the Cordillera.

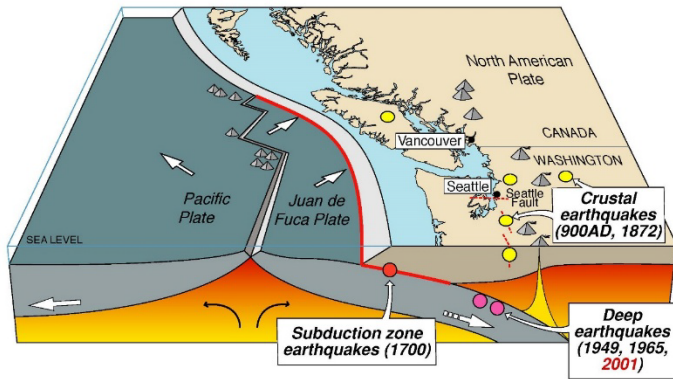


FIGURE 2: CASCADIA SUBDUCTION ZONE SEISMOTECTONIC SETTING. IMAGE SOURCE: USGS.

The pipeline owner's objectives were to (1) estimate the annual system-wide risk of pipeline rupture or facility damage due to seismicity and co-seismic processes, and (2) identify locations that contributed most to the total system-wide annual hazard, such that they could be prioritized for risk reduction measures. The work builds upon earlier efforts to map terrain susceptible to co-seismic ground failure and develop earthquake monitoring and response systems.

The project benefitted from extensive subsurface geotechnical information, including approximately 1700 boreholes; and project-specific terrain maps that classified geological deposit types and geomorphic processes. Available borehole data included SPT blow counts, shear vanes, Atterberg limits, and grain size distributions. Boreholes were more densely spaced at crossings of watercourses, roads, railroads, and known areas of slope instability, and otherwise relatively sparse.

3. OVERVIEW OF PROCEDURES

The following workflow was implemented for co-seismic landslide hazard sites:

- 1) Inventory potential hazard sites.
- 2) Calculate the seismic resistance of the slope (i.e., critical acceleration, a_c)
- 3) Perform probabilistic seismic hazard analyses
- 4) Perform a screening-level assessment using a pseudo-probabilistic approach at 1/2475 annual exceedance probability (AEP)
- 5) Develop displacement hazard curves for site with non-negligible displacement determined in the screening-level assessment
- 6) Perform pipe-soil interaction analysis to develop pipeline strain response curves.
- 7) Estimate probability of pipeline failure as a function of pipe strain.
- 8) Calculate the vulnerability of the pipeline at various seismic hazard return periods to develop a pipeline failure hazard curve.

The following workflow was implemented for lateral spreading hazard sites:

- 1) Inventory potential hazard sites.
- 2) Perform probabilistic seismic hazard analyses
- 3) Calculate probability of triggering liquefaction, screening sites where liquefaction triggering probability is negligible at 1/2475 AEP.
- 4) Develop lateral displacement hazard curves for sites passing the screening-level assessment.
- 5) Perform pipe-soil interaction analysis to develop pipeline strain response curves.
- 6) Estimate probability of pipeline failure as a function of pipe strain.
- 7) Calculate the vulnerability of the pipeline at various seismic hazard return periods.

Holocene fault crossings are absent along the pipeline corridor; accordingly, faulting was excluded from the work scope.

4. CO-SEISMIC GEOHAZARD INVENTORY

Regional scale hazard assessments typically involve applying a SDPM on a grid basis across a wide area; however, this is computationally intensive and introduces challenges with selecting a representative landslide or lateral spreading zone that could impact the linear infrastructure. In this study, sites with potential for co-seismic landslides or lateral spreading hazards were first inventoried along the full pipeline corridor to limit detailed further analyses to crossings with non-negligible pipeline failure probabilities.

To delineate hazard sites associated with potential co-seismic landslides, critical accelerations were estimated using a generalized shear-strength model and an assumed infinite-slope landslide mechanism [13, 14]. The shear strength model classifies geological units into three general groups, each of which is assigned an assumed friction angle and cohesion intercept. Project-specific terrain maps and published bedrock geological maps were the basis for geologic group assignments. A larger number of groups may improve local accuracy but for a system-wide probabilistic screening, broad categories balance resolution with feasibility. Critical acceleration was calculated using an infinite-slope model with assumed slip-surface depth of 3 m, assumed wet conditions (i.e., groundwater height at 2.4 m above the slip surface), and slope angle derived from a 25 m resolution digital elevation model. Potential co-seismic landslide sites were included in an inventory where calculated critical acceleration was generally less than 0.15 g and the slope angle exceeded 8° [15]. Approximately 300 landslide sites were inventoried using this process.

The inventory of lateral spreading sites was based on qualitative liquefaction susceptibility classes, which are in turn informed by geological deposit type and age [10, 11]. Lateral spreading hazard sites were inventoried where the qualitative susceptibility rating was equal to or greater than 'high' (when using [11]) or "moderate to high" (when using [11]) and within 250 m of a free face [1] or on ground steeper than 0.5° [16].

Approximately 170 lateral spreading sites were inventoried using this process and used for the screening level assessment

5. SCREENING-LEVEL ASSESSMENTS

To further focus the study, a screening-level pseudo-probabilistic assessment was performed. For co-seismic landslide hazard sites, the screening-level assessment involved calculating median displacement magnitudes at a 1/2475 AEP hazard level. This hazard level corresponds to a typical design basis for critical infrastructure in USA (ASCE 7) and Canada (NBCC). Furthermore, this hazard level was selected as the pipeline operator's desired design basis for other components of their pipeline system. A probabilistic seismic hazard assessment (PSHA) using the 6th Generation National Building Code of Canada seismic hazard model [17, 18] was performed at each site to obtain uniform hazard response spectra (UHRS) and disaggregation of the seismic hazard. SDPMs were implemented for crustal [19, 20] and subduction [21] tectonic regions. A key input into the SDPM is a_c (also known as yield acceleration [k_y]).

5.1. Automated Stability Modelling

The typical approach for calculating a_c on a site-specific basis is to use a limit equilibrium slope stability model that satisfies three equilibrium equations: moments, forces in the vertical direction, and forces in the horizontal direction. However, limitations arise when having to perform hundreds of slope stability runs over a range of material types, slope angles, and water table levels. When performing seismic slope stability modelling on a regional scale, an infinite-slope limit equilibrium model is typically used given the simplicity of the calculation [13, 22]. However, this model is generally applicable only to slopes composed of homogenous cohesionless soil, where the slip surface is shallow and parallel to the slope face [23]. Limitations also arise when having to estimate the fundamental period of the landsliding mass (T_s) and for selecting a representative slope which could impact the pipeline. Given these limitations, a more robust limit-equilibrium model was desired. As such, BGC used an open-source python program called Pyslope [24], which performs limit equilibrium stability modelling based on the simplified Bishop procedure. Modifications were made to the python code to accommodate undrained shear strength ratios and application of a horizontal seismic load (k_h). Helper python scripts were developed to automate setting the soil parameters, slope height and angle, water table, and calculation of a_c .

To capture epistemic uncertainty in the soil strength models and groundwater levels used in the stability modelling, a logic tree approach was implemented [25] (Figure 4). For each site and associated landslide slope, up to twelve a_c values were calculated. Undrained shear strength parameters were used for fine-grained soil deposits. Drained strength parameters were used for coarse-grained soil deposits.

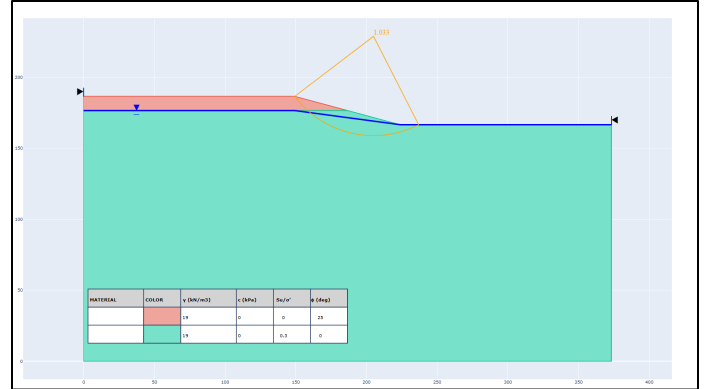


FIGURE 3: EXAMPLE OUTPUT OF A STABILITY MODEL FOR A FINE-GRAINED MATERIAL TYPE.

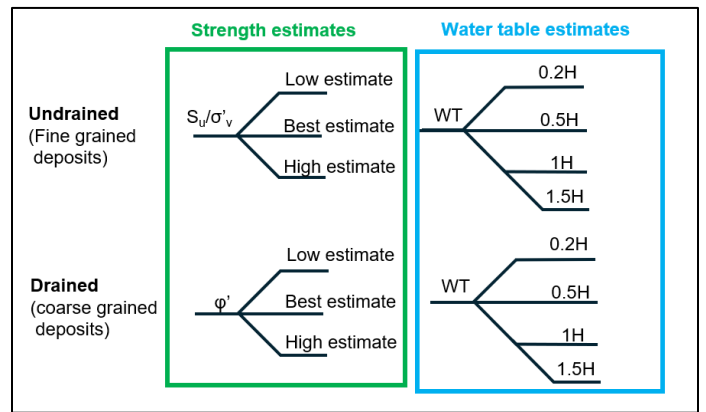


FIGURE 4: LOGIC TREE APPROACH FOR CALCULATING a_c . H IS EQUAL TO THE HEIGHT OF THE SLOPE AND WATER TABLE DEPTH (WT) WAS MEASURED RELATIVE TO THE CREST OF THE SLOPE.

Soil strength parameters were correlated to project-specific terrain mapped surficial material types using available borehole data in the area. Available borehole data included SPT blow counts, shear vanes, Atterberg limits, and grain size distributions, with approximately 1700 boreholes available. Logic-tree weighting ensured that epistemic uncertainty was represented rather than relying on single deterministic values.

Weightings were applied to each calculated a_c based on a log-normal distribution by calculating the mean and standard deviation of calculated a_c values associated with each site and landslide slope.

An additional output from stability modelling included calculating the initial fundamental period of the sliding mass (T_s), which is a required input into the SDPM [20, 21].

$$T_s = \frac{4H}{V_s}$$

The soil parameters and dynamic response were used along with simplified procedures to estimate displacements induced by liquefaction and landslides.

5.2. Pseudo-Probabilistic Displacement Modelling for Landslides

Using the inputs from the stability modelling, SDPM for crustal [20] and subduction [21] earthquakes were applied to estimate displacements for each site at a 1/2475 AEP seismic hazard level. Spectral accelerations (SA) were obtained at degraded fundamental periods of 1.3T from the total UHRS. Mean magnitudes for each tectonic region type (crustal and subduction) were obtained from disaggregations of the 1/2475 hazard level ground motions and used to calculate tectonic region-specific displacement magnitudes. The scalar model was used for crustal tectonic region types while the vector model (based on two intensity measure types) was used where peak ground velocity (PGV) exceeded 40 cm/s for interface earthquakes and 20 cm/s for intraslab earthquakes [21]. The total displacement associated with the median displacement prediction from each tectonic region was calculated using a weighted average approach, where the percent contribution to the total hazard was used as a weighting factor. The displacements associated with each realization of the stability model logic tree (Figure 4) were then aggregated using the weightings of each a_i to provide a total displacement magnitude for each site. Sites with less than a 5 cm median displacement magnitude threshold were removed from subsequent fragility analysis (Figure 5).

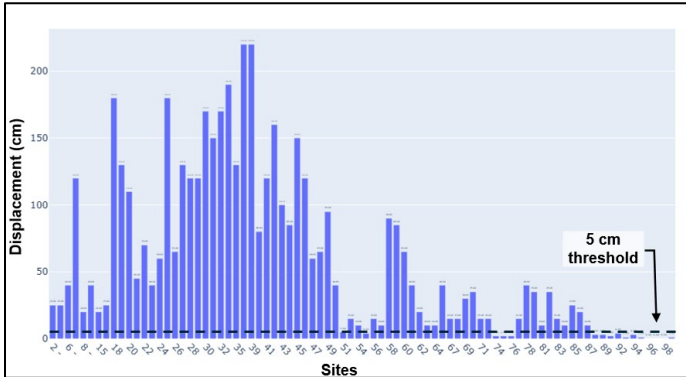


FIGURE 5: BAR CHART EXAMPLE OF PSEUDO-PROBABILISTIC DISPLACEMENT RESULTS FOR A SUBSET OF INVENTORIED SITES.

5.3. Liquefaction Triggering Analysis

For the screening-level analysis of lateral spreading sites, probability of triggering liquefaction was calculated using [26] where borehole data were available, and using Federal Emergency Management Agency (FEMA) criteria [22] for sites without available borehole data. The seismic hazard level used in the screening-level analysis was PGA at 1/2475 AEP, similar to the co-seismic landslide sites. In general, sites with a probability of triggering liquefaction greater than 0.05 were included for further analysis (e.g., development of displacement hazard curves and pipeline fragility).

6. PROBABILISTIC DISPLACEMENT ANALYSIS

While the 1/2475 AEP level offers a useful benchmark for preliminary decision-making, a full probabilistic hazard curve provides a more comprehensive basis for analysis. By considering the entire range of exceedance probabilities, probabilistic curves capture the spectrum of possible outcomes and enable more robust risk assessments.

Probabilistic hazard curves for lateral spreading and landslide displacement are grounded on the PEER performance-based framework [27], defined by:

$$\lambda(DV) = \iiint G(DV|DM)dG(DM|EDP)dG(EDP|IM)d\lambda(IM)$$

Where $\lambda(DV)$ is the mean annual rate of exceedance of a decision variable (DV), DM is a damage measure, EDP is an engineering demand parameter, IM is an intensity measure, and the terms in the equation are conditional probabilities independent of one another.

To obtain displacement hazard curves, where displacement is the EDP, additional conditional probabilities should be considered to include the conditional disaggregation of the ground motion hazard and rate of occurrence.

The seismic hazard underpinning the lateral spreading and landslide displacement analysis can be computed using the OpenQuake engine. This tool provides hazard curves and disaggregation data, classified by tectonic region (crustal and subduction: interface and intraslab).

6.1. Landslide displacement hazard curves

The procedure to estimate probabilistic landslide displacement hazard curves (DHC) consists of solving this equation [28]:

$$\lambda(D > d) = \iint \lambda(IM) \cdot P(D > d|IM, M, k_y, T_s) \cdot P(M|IM)\Delta\lambda(IM)d(IM)d(M)$$

Where $\lambda(D > d)$ is the annual rate of exceedance of a threshold displacement d , M is magnitude, k_y is the yield acceleration, T_s is the initial fundamental period, and IM is the spectral acceleration at a degraded period $1.3T_s$ ($Sa(1.3T_s)$).

- 1) Each site's response spectrum is interpolated to estimate $Sa(1.3T_s)$ values at selected return periods.
- 2) Then, conditional probabilities of slope displacement, $P(D > d|IM)$, are computed per return period using the disaggregated M and tectonic region-specific ground motion levels for crustal [20] and subduction [21] earthquakes.
- 3) For each return period, the conditional probabilities are weighted by the disaggregation contributions and by the weights (w_{k_y}) assigned to k_y in the logic tree, to calculate $\sum P(D > d|IM, M, k_y, T_s) \cdot P(M|IM) \cdot w_{k_y}$
- 4) For each tectonic region, the rate of occurrence, $\Delta\lambda(IM)d(IM)$, is calculated to obtain DHC for each source type and IM.
- 5) In the last stage, the DHC are calculated by aggregating the DHCs for each tectonic region within each displacement bin.

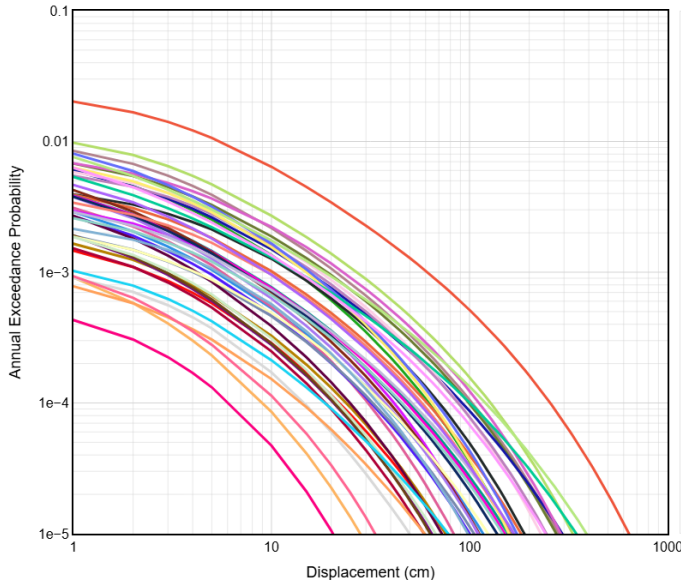


FIGURE 6: EXAMPLE OF A SERIES OF DHCS ASSOCIATED WITH CO-SEISMIC LANDSLIDE HAZARD SITES.

6.2. Lateral spreading displacement hazard curves

A lateral displacement prediction equation that can be separated into two parts was used [16]. One is the loading parameter (L) which is dependent on magnitude (M) and source-to-site distance (R) and the other is a site parameter (S) dependent on site specific conditions (e.g., $N_{1(60)}$, thickness of liquefiable unit, grain size, free-face height, and/or slope gradient, etc.), and ε represents uncertainty:

$$\log D_H = L - S + \varepsilon$$

The loading part (L) can be used as an IM:

$$L = b_1 M + b_2 \log R^* + b_3 R$$

Where b_1 , b_2 , and b_3 are regression coefficients and R^* is a distance parameter for near-source earthquakes

A probabilistic framework for lateral spreading, solving the following equation, was used [29]:

$$\lambda_{D_H}(d|S) = \sum \lambda(M|m) \sum \sum P(D_H > d|S, M = m, R = r) \cdot P(M = m, R = r)$$

Where $\lambda(M|m)$ is the mean annual rate of exceeding a minimum magnitude of interest for a given seismic source.

- 1) L is calculated from the disaggregated M , R values using a lognormal standard deviation.
- 2) Computed L values are used to generate exceedance probabilities across a range of thresholds (i.e., $P(L > l)$) using the cumulative distribution function.
- 3) Following the PEER framework, the joint probability distribution of L is calculated by weighting M and R by disaggregation contributions.
- 4) L values are translated into expected displacements with the site parameters. When borehole data was available at a site, site parameters were calculated for each borehole and a weight was assigned (generally an

average). When borehole data was unavailable, three-point distribution of site parameters for each liquefaction susceptibility rating was applied and weighted according to a normal distribution.

- 5) Resulting displacement estimates were aggregated based on weightings for each site to produce a single displacement hazard curve.

7. RESULTS AND DISCUSSION

The approach described herein will yield seismic displacement hazard curves at each co-seismic landsliding and lateral spreading hazard crossing that meets the 1/2475 AEP screening threshold: median displacement exceeding 5 cm for landslides, and liquefaction probability exceeding 5% for lateral spreading sites. Once seismic displacement hazard curves are established for these sites, the next step would be to incorporate a vulnerability assessment. This could be performed at each site using screening-level criteria [4], but given the complexity arising for variable geometry at each crossing (e.g., burial depths, orientation of the pipeline with respect to the expected ground movement direction, length of pipe embedded in moving ground), a more appropriate approach would be to develop fragility curves on a site-by-site basis using finite-element modelling. At this time, the development of fragility curves remains in progress and will be the subject of future work.

The methodology described herein makes several simplifying assumptions. First, the geology of co-seismic geohazard sites is generally assumed to be uniform. Second, shear-strength values are assumed to be consistent within mapped geological units, in which logic trees capture epistemic uncertainty in shear-strength values. Accordingly, each unit is represented by a range of potential shear-strength values, rather than a single value based on observed conditions (i.e., from boreholes and geotechnical testing at every location). Third, conservative site-classes were used when performing PSHAs. Fourth, the approach uses simplified limit-equilibrium models with simplified stratigraphy, and semi-empirical and empirical seismic displacement prediction models. It is expected that pipeline rupture probability might be inaccurate on a site-by-site basis, but that the aggregated risk across the pipeline system should be relatively representative. As such, locations that are identified as having an elevated likelihood of experiencing large ground displacements, or, after the next stage of developing fragility models, would have an elevated probability of failure, would be best assessed by reducing uncertainty in the input shear strength model through site-specific geotechnical studies, and/or replacing empirical DPMs with site-specific displacement analysis.

8. CONCLUSION

The approach described in this paper represents a first step in analyzing system-wide seismic risk. It describes the geotechnical hazard analysis component; specifically, the development of seismic displacement hazard curves for pipeline crossings. Subsequent work will integrate vulnerability models to enable a system-wide risk analysis. The method can help

operators prioritize mitigation, improve repair and replacement protocols, and allocate post-earthquake geotechnical investigations more cost-effectively. System wide failure estimates can directly inform budgets and regulatory compliance.

ACKNOWLEDGEMENTS

The project benefitted from review by Dr. Saman Zarnani of BGC Engineering and Dr. Jorge Macedo of Georgia Tech University. This paper was improved following thoughtful and constructive reviews by three anonymous reviewers nominated by the conference committee.

REFERENCES

- [1] O'Rourke, M.J., & Liu, X., (1999). *Response of Buried Pipelines Subjected to Earthquake Effects*. MCEER Monograph, 3. University of New York at Buffalo, US.
- [2] Lanzano, G, E. Salzano, F. Santucci de Magistris, and G. Fabbrocino. 2014. "Seismic vulnerability of gas and liquid buried pipelines." *J. Loss Preven. Process Ind.* 28, 72-78. <http://dx.doi.org/10.1016/j.jlp.2013.03.010>.
- [3] Nyman, D., and G. Bouckovalas, 2019. "Assessment and Mitigation of Seismic Geohazards for Pipelines." In *Pipeline Geohazards: Planning, Design, Construction and Operations*, edited by M. Rizkalla and R.S. Read. ASME Press. https://doi.org/10.1115/1.861790_ch11.
- [4] Lanzano, G., F. Santucci de Magistris, G. Fabbrocino,, and E. Salzano. 2015. "Seismic damage to pipelines in the framework of Na-Tech risk assessment." *J. Loss Prev. Process Ind.* 33, 159–172. <https://doi.org/10.1016/j.jlp.2014.12.006>.
- [5] Baize, S., F. Nurminen, A. Sarmiento, et al. 2020. "A Worldwide and Unified Database of Surface Ruptures (SURE) for Fault Displacement Hazard Analysis." *Seismol. Res. Lett.* 91 (1), 499-520. <https://doi.org/10.1785/0220190144>.
- [6] Santucci de Magistris, F., G. Lanzano, G. Forte, and G. Fabbrocino. 2013. "A database for PGA threshold in liquefaction occurrence." *Soil Dyn. Earthq. Eng.* 54, 17-19. <https://doi.org/10.1016/j.soildyn.2013.07.011>.
- [7] Ambraseys, N. (1988). "Engineering Seismology." *Earthq. Eng. Struct. Dyn.* 17(1), 1-50. <https://doi.org/10.1002/eqe.4290170101>.
- [8] Green, R.A., and J.J. Bommer. 2019. "What is the smallest earthquake magnitude that needs to be considered in assessing liquefaction hazard?" *Earthq. Spectra* 35, 1441-1464. <https://doi.org/10.1193/032218EQS064M>.
- [9] Honegger, D.G., D.J. Nyman, and T.L. Youd. 2006. "Liquefaction hazard mitigation for oil and gas pipelines," paper presented at 8NCEE, San Francisco, CA, April 18-22. EERI.
- [10] Youd, T.L., and D.M. Perkins. 1978. "Mapping of liquefaction induced ground failure potential." *J. Geotech. Eng.* 104 (4), 433-446. <https://doi.org/10.1061/AJGEB6.0000612>.
- [11] Quinn, P., M. Zaleski, R. Mayfield, H. Karimian, and B. Waddington. 2015. "Liquefaction susceptibility mapping derived from terrain mapping; experience on a linear project in British Columbia, Canada," paper presented at GEOQuébec, Quebec, QC, September 20-23. CGS.
- [12] Honegger, D., and D. Nyman. 2017. "Pipeline seismic design and assessment guideline." PRCI Technical Report PR-268-134501-R01. <https://doi.org/10.55274/R0011445>.
- [13] Wieczorek, G.F., Wilson, R.C., and Harp, E.L. (1985) *Map showing slope stability during earthquakes in San Mateo County California*, scale 1:62,500. USGS Miscellaneous Investigations Map I-1257-E. <https://doi.org/10.3133/i1257E>.
- [14] Wilson, R.C., and Keefer, D.K. (1985). Predicting areal limits of earthquake-induced landsliding. In *Evaluating Earthquake Hazards in the Los Angeles Region—An Earth-Science Perspective*, edited by J.I. Ziony. USGS Professional Paper 1360. <https://doi.org/10.3133/pp1360>.
- [15] Rodriguez, C.E., J.J. Bommer, and R.J. Chandler. 1999. "Earthquake-induced landslides: 1980-1997." *Soil Dyn. Earthq. Eng.* 18 (5), 325-346. [https://doi.org/10.1016/S0267-7261\(99\)00012-3](https://doi.org/10.1016/S0267-7261(99)00012-3).
- [16] Youd, T.L., C.M. Hansen, and S.F. Bartlett. 2002 "Revised multilinear regression equations for prediction of lateral spread displacement." *J. Geotech. Geoenviron. Eng.* 128 (12), 1007–1017. [https://doi.org/10.1061/\(ASCE\)1090-0241\(2002\)128:12\(1007\)](https://doi.org/10.1061/(ASCE)1090-0241(2002)128:12(1007)).
- [17] Adams, J., T. Allen, S. Halchuk, and M. Kolaj. 2019. "Canada's 6th Generation Seismic Hazard Model, as Prepared for the 2020 National Building Code of Canada", paper presented at 12th CCEE, Quebec, June 17-20. CAEE.
- [18] Kolaj, M., S.C. Halchuk, and J. Adams. 2023. *Sixth Generation seismic hazard model of Canada: final input files used to generate the 2020 National Building Code of Canada seismic hazard values*, version 1.0. GSC Open File 8924. <https://doi.org/10.4095/331387>.
- [19] Bray, J.D., and J. Macedo. 2019. "Closure to "Procedure for Estimating Shear-Induced Seismic Slope Displacement for Shallow Crustal Earthquakes" by Jonathan D. Bray and Jorge Macedo." *J. Geotech. Geoenviron. Eng.* 145 (12), 07021007. [https://doi.org/10.1061/\(ASCE\)GT.1943-5606.0002499](https://doi.org/10.1061/(ASCE)GT.1943-5606.0002499).
- [20] Bray J.D., and J. Macedo. 2019b. "Procedure for estimating shear-induced seismic slope displacement for shallow crustal earthquakes." *J. Geotech. Geoenviron. Eng.* 145 (12), 04019106. [https://doi.org/10.1061/\(ASCE\)GT.1943-5606.0002143](https://doi.org/10.1061/(ASCE)GT.1943-5606.0002143).
- [21] Macedo, J., J.D. Bray, and C. Liu. 2023. "Seismic slope displacement procedure for interface and intraslab subduction zone earthquakes." *J. Geotech. Geoenviron. Eng.* 149 (11), 04023104. <https://doi.org/10.1061/JGGEFK.GTENG-11445>.
- [22] Federal Emergency Management Agency. 2024. "Hazus Earthquake Model Technical Manual", Version 6.1. U.S. Department of Homeland Security.
- [23] Duncan, J., S. Wright, and T. Brandon. 2014. *Soil strength and slope stability*, 2nd edition. John Wiley and Sons.
- [24] Bonanno, J. 2022. "PySlope: Python-based slope stability analysis." <https://github.com/JesseBonanno/PySlope>.
- [25] Ojomo, O., E. Rathje, P. Wang, et al. 2024. "Regional earthquake-induced landslide assessments for use in seismic risk analyses of distributed gas infrastructure systems." *Eng. Geol.* 340, 107664. <https://doi.org/10.1016/j.enggeo.2024.107664>.

[26] Boulanger, R.W., and I.M. Idriss. 2012. “Probabilistic Standard Penetration Test-based liquefaction triggering procedure.” *J. Geotech. Geoenviron. Eng.*, 138 (10), 1185–1195. [https://doi.org/10.1061/\(ASCE\)GT.1943-5606.0000700](https://doi.org/10.1061/(ASCE)GT.1943-5606.0000700).

[27] Deierlein, G.G., H. Krawinkler, and C.A. Cornell. 2003. “A framework for performance-based earthquake engineering,” paper presented at PCEE, Christchurch, NZ, February 13-15.

[28] Bray, J.D., and J. Macedo, J. 2023. Performance-based seismic assessment of slope systems. *Soil Dyn. Earthq. Eng.*, 168, 107835. <https://doi.org/10.1016/j.soildyn.2023.107835>.

[29] Franke, K.W., and S.L. Kramer. 2013. “Procedure for the empirical evaluation of lateral spread displacement hazard curves.” *J. Geotech. Geoenviron. Eng.* 140 (1), 110-120. [https://doi.org/10.1061/\(ASCE\)GT.1943-5606.0000969](https://doi.org/10.1061/(ASCE)GT.1943-5606.0000969).